NORWEGIAN JOURNAL OF GEOLOGY
https://dx.doi.org/10.1785/njg100-4-4

GEOLOGICAL SOCIETY OF NORWAY

Tectono-sedimentary evolution of the eastern Forlandsundet Graben, Svalbard

Niklas W. Schaaf[1,2,3], Per Terje Osmundsen[4,2], Roelant Van der Lelij[5], Jasmin Schönenberger[5], Olaf K. Lenz[6,7], Tim Redfield[5] and Kim Senger[1]

[1] *Department of Arctic Geology, The University Centre in Svalbard, 9171 Longyearbyen, Norway*
[2] *Department of Geosciences, University of Oslo, 0316 Oslo, Norway*
[3] *current affiliation: Institute of Geosciences, Kiel University, 24118 Kiel, Germany*
[4] *Department of Geoscience and Petroleum, Norwegian University of Science and Technology, 7491 Trondheim, Norway*
[5] *Geological Survey of Norway, 7491 Trondheim, Norway*
[6] *Institute of Applied Geosciences, Technical University of Darmstadt, 64287 Darmstadt, Germany*
[7] *Senckenberg Society for Nature Research, 60325 Frankfurt, Germany*

E-mail corresponding author (Niklas W. Schaaf): niklas.schaaf@ifg.uni-kiel.de

Keywords:
- *Spitsbergen*
- *Transform margin*
- *Oblique rifting*
- *Extensional tectonics*
- *Transtension*
- *Transpression*

- *Electronic Supplement 1: Zircon fission track data*
- *Electronic Supplement 2: Apatite fission track data*
- *Electronic Supplement 3: Lithofacies description*
- *Electronic Supplement 4: Lithological logs*
- *Electronic Supplement 5: Sarstangen lithofacies*
- *Electronic Supplement 6: Lithological log*
- *Electronic Supplement 7: Palynostratigraphic analysis*

Received:
5. May 2020

Accepted:
7. December 2020

Published online:
10. March 2021

The Forlandsundet Graben, situated along the NE Atlantic continental margin in the western Svalbard archipelago in Arctic Norway, represents a unique opportunity to study a basin that evolved along an obliquely rifted margin. It is bound by N–S-trending fault zones that cross-cut the structures of the Eocene West Spitsbergen-fold-and-thrust-belt. The basin fill comprises coarse continent-derived siliciclastics and finer-grained marine deposits. The Forlandsundet Graben is a keystone to understand the evolution of the west Svalbard margin from a transpressional fold-and-thrust-belt to a sharply tapered transtensional margin during the Paleogene. We report data collected during three field seasons at the eastern basin margin, including outcrop descriptions, ~500 structural measurements, ~370 m of sedimentary logs, more than 100 paleocurrent indicators and results from palynology, K–Ar dating and apatite fission track thermochronology. Our results suggest that the basement units along the eastern basin boundary experienced reverse faulting and illite growth in a fault gouge at 53.5 ± 1.0 Ma likely related to the Eurekan orogeny. This transpressional phase was followed by NW–SE transtensional rifting which initiated the oblique normal faults that constitute the present eastern basin boundary. In this setting, the sedimentary units on Sarsøyra were deposited. The older Sarsbukta conglomerate comprises interfingering alluvial-fan and fluvial deposits. It was affected by transtensional folding and faulting. The rocks of the younger Sarstangen conglomerate record basin-floor and fan-delta sedimentation and thus transition to marine deposition along a major intrabasinal normal or oblique fault. Palynostratigraphic analyses suggest an Early to Middle Oligocene age for the Sarstangen conglomerate. Our findings further highlight a maturity discrepancy between the sedimentary deposits along the eastern and western basin boundaries. On this basis, we discuss possible basin models, including the evolution of the Forlandsundet Graben in association with a metamorphic core complex.

Niklas W. Schaaf, Per Terje Osmundsen, Roelant Van der Lelij, Jasmin Schönenberger, Olaf K. Lenz, Tim Redfield and Kim Senger: Tectono-sedimentary evolution of the eastern Forlandsundet Graben, Svalbard. *Norwegian Journal of Geology 100,* 202021. https://dx.doi.org/10.17850/njg100–4–4.

Introduction

The evolution of continental rifts into passive continental margins is a matter of ongoing debate that focuses much on orthogonally rifted segments (e.g., Peron-Pinvidic et al., 2013; Brune et al., 2018; Osmundsen & Péron-Pinvidic, 2018). Oblique rifting, however, may result in more complex tectonic and sedimentary architectures. Basins that formed during the development of the Barents Sea transform margin show such characteristics (Kristensen et al., 2017). The west Svalbard margin (WSM) is the northern continuation of the west Barents Sea margin and formed with the opening of the Norwegian–Greenland Sea under similar tectonic conditions (Faleide et al., 2008). With a combined length of approximately 1500 km, they constitute one of the longest transform margin segments worldwide (Fig. 1B; Blinova et al., 2009). The understudied Forlandsundet Graben (FG; Fig. 1B) evolved in response to passive margin formation along the WSM (Gabrielsen et al., 1992; Ritzmann et al., 2004; Kleinspehn & Teyssier, 2016). It is located on, and between, the islands Prins Karls Forland (PKF) and Spitsbergen (Fig. 1B) in the westernmost part of the Svalbard archipelago. The FG occupies a key position to investigate processes that occur during continental breakup and represents a rare onshore analogue for basins preserved offshore along obliquely rifted margins (e.g., Sutherland et al., 2012; Díaz-Azpiroz et al., 2016; Kristensen et al., 2017).

Despite limited scientific attention, a small number of studies provide a framework for the tectonic (Steel et al., 1985; Lepvrier, 1990; Gabrielsen et al., 1992; Kleinspehn & Teyssier, 1992, 2016; Krasilscikov et al., 1995; Bergh et al., 1999; von Gosen & Paech, 2001; Blinova et al., 2009; Schneider et al., 2018), stratigraphic (Manum, 1962; Lehmann et al., 1978; Rye-Larsen, 1982; Manum & Throndsen, 1986; Čepek, 2001; Čepek & Krutzsch, 2001) and thermal (Paech & Koch, 2001; Barnes & Schneider, 2018) evolution of the FG. The geological history of the FG does, however, remain enigmatic due to a series of unresolved structural, sedimentological and geochronological problems. One is the lack of a detailed and updated sedimentological description that can complement and refine the existing basin-wide stratigraphic characterisation (e.g., Rye-Larsen, 1982). Furthermore, the correlation between the eastern and western parts of the sedimentary fill is poor. A major concern here is related to reliable stratigraphic ages. On the tectonic side, a fundamental question is related to whether the FG formed under progressive transtension entirely or if parts of its sedimentary record experienced compression during the Eurekan orogeny (Fig. 1C; Bergh et al., 1997; Braathen et al., 1997; Piepjohn et al., 2016). An E–W gradient in structural complexity and thermal maturity across the basin that could help address this issue has received little recognition so far. From a structural point of view, the FG contains a complex assemblage of compressional and extensional features. The relationships between them are unclear due to an insufficient understanding of the deformation sequence and its timing. Thus, we recognise the following knowledge gaps:

- Detailed and well-documented sedimentological descriptions of the basin fill.
- Precise ages of the sedimentary strata.
- A sufficient kinematic database.
- Dating of tectonic events.

This study aims to provide a solid documentation of the structural and sedimentary features along the eastern margin of the FG. In addition to the collection of structural and sedimentological data, we sampled basement rocks for apatite fission-track analysis, clay-bearing fault gouge for K–Ar analysis and fine-grained sediments as well as coal for palynological analysis (see Fig. 2A for locations of field area and sample locations). More specifically, we address the identified knowledge gaps using:

- 370 m of sedimentological logs, measured by us and supplemented by detailed outcrop drawings and palynological analyses.

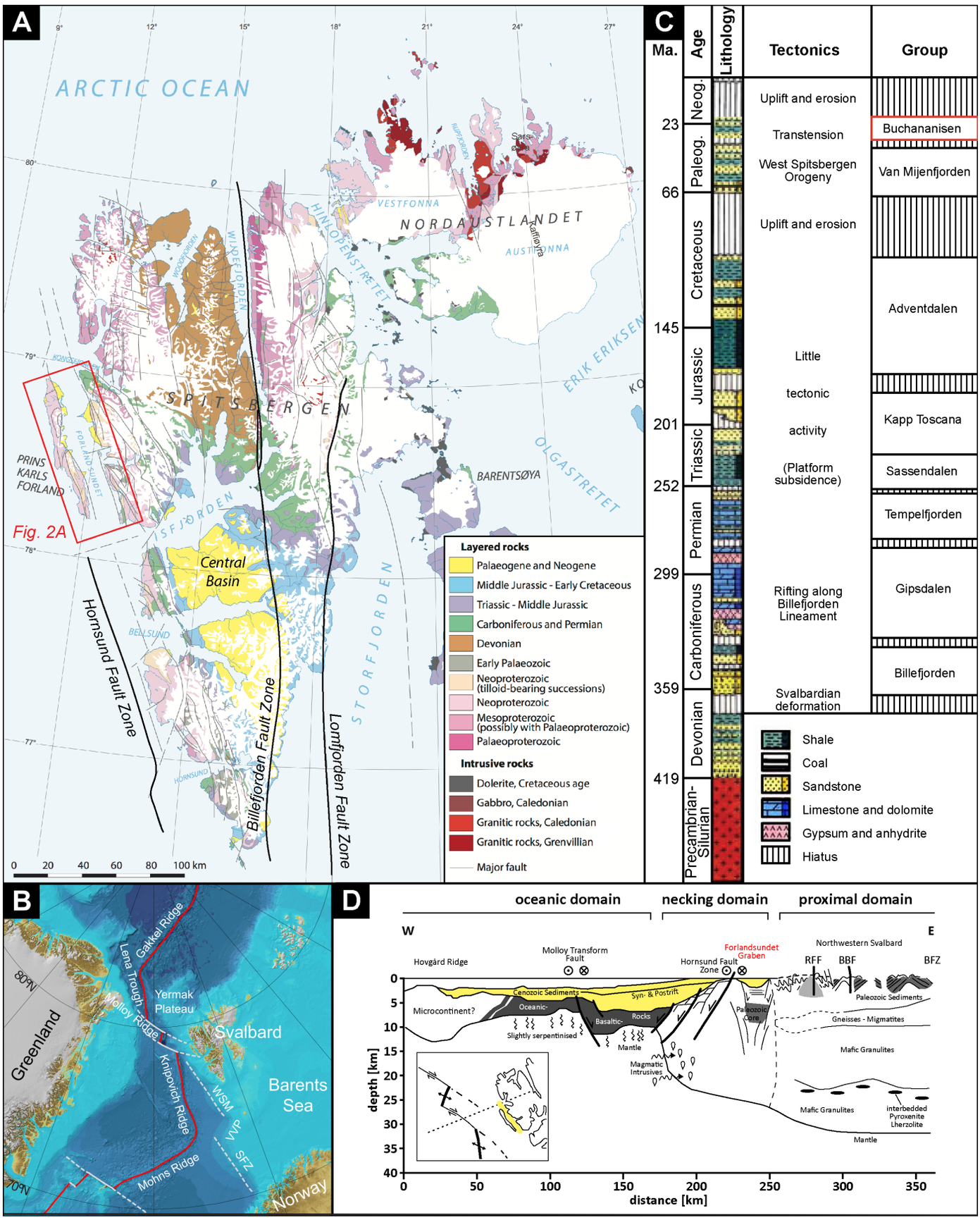

Figure 1. (A) Simplified geological map of Svalbard with the location of the Forlandsundet Graben (FG; modified from Dallmann et al., 2015). (B) Location of Svalbard with the present configuration of the west Barents Sea margin; WSM – west Svalbard margin, VPP – Vestbakken Volcanic Province and SFZ – Senja Fracture Zone. The bathymetric map is from Jakobsson et al. (2012). (C) Summary of the tectonic history and the associated sedimentary deposits on Svalbard (modified from Nøttvedt et al., 1993). The sedimentary units assessed in this study are part of the Buchananisen Group (highlighted in red). (D) Interpretation of a seismic refraction profile across the Svalbard margin north of the FG (redrawn and modified from Ritzmann et al., 2004). Note the sharply tapered crust and a Moho that shallows from more than 30 km to less than 10 km over a short distance of c. 100 km; RFF – Raudfjorden Fault, BBF – Breibogen Fault, BFZ – Billefjorden Fault Zone. See inset map, where the FG is indicated in yellow, for location of the section.

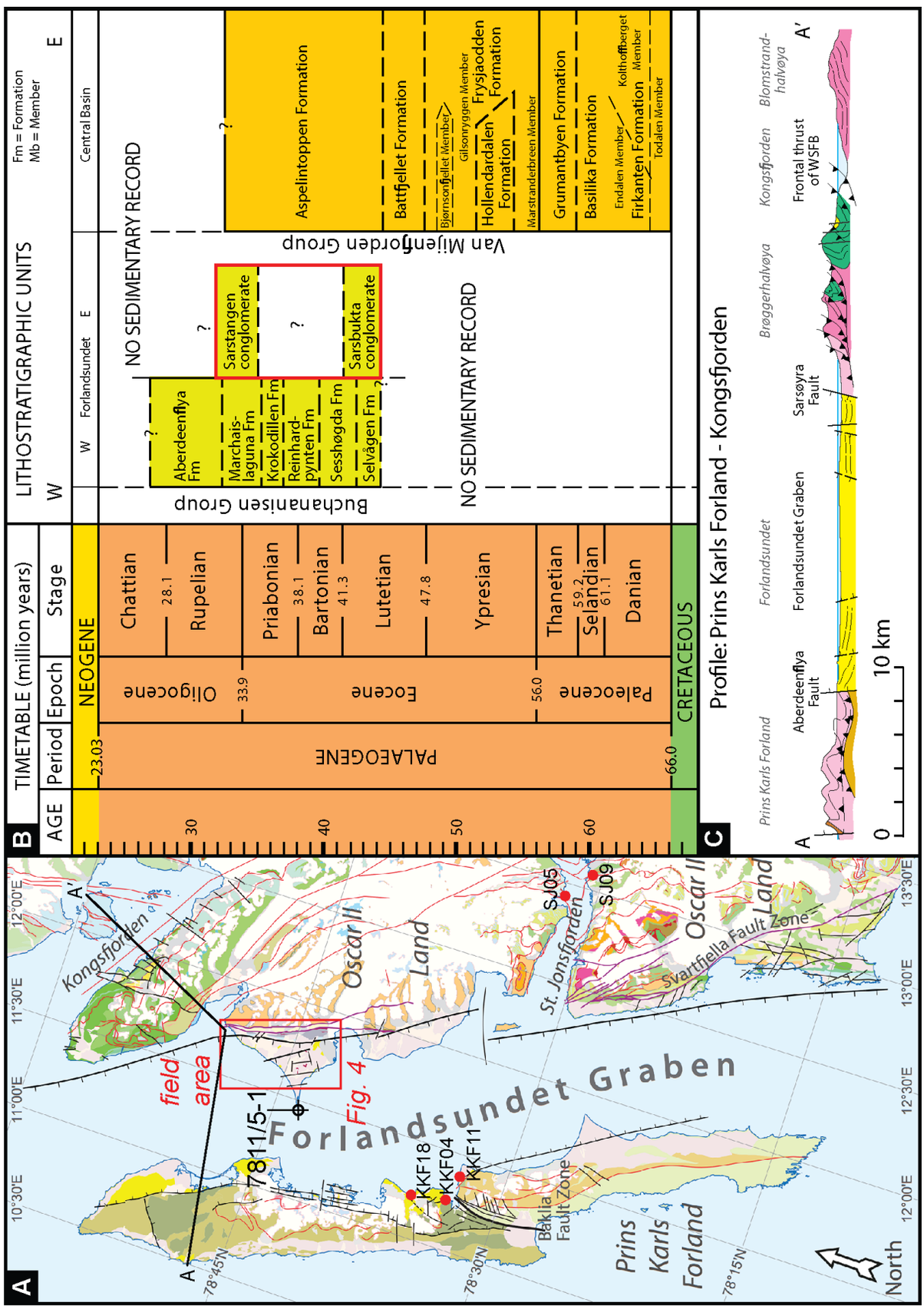

Figure 2. (A) Location of the study area in Sarsøyra (red rectangle) on a simplified geological map of the Forlandsundet Graben (FG; modified from Dallmann et al, 2015). Red dots mark the sample locations for fission track thermochronology in St. Jonsfjorden and on Prins Karls Forland (PKF). The location of the map is indicated by the red rectangle in Fig. 1A. (B) Summary of the Paleogene stratigraphy of the FG and the Central Basin (modified from Dallmann et al, 2015). The sedimentary units assessed in this study are marked with a red rectangle. (C) Cross-section across the northern part of the PKF, the FG and the WSFB (from Dallmann et al, 2015). Vertical exaggeration is 200%. The location of the cross-section (A–A') is marked by the black line in (A).

• ~500 structural measurements from the metamorphic basement and Paleogene sedimentary units.
• X–ray diffraction (XRD) analyses and K–Ar dating of a fault gouge within the basement units close to the basin boundary.
• Apatite and zircon fission track thermochronology on samples from western Spitsbergen and PKF (Fig. 2A).

Our results offer new constraints for the tectono-sedimentary evolution of the eastern FG, and we discuss their implications with respect to the overall basin history. The FG represents a basin that developed along an obliquely deformed margin, with major changes in the local strain field over time. As such, it may provide an important analogue for basins adjacent to other parts of the west Barents Sea margin, and obliquely rifted margin segments elsewhere.

Geological background

The Norwegian Svalbard archipelago comprises all islands in the high Arctic between 74° to 81°N and 10° to 35°E (Fig. 1B). Since 540 Ma, Svalbard drifted from 40° S to its present position, accumulating a diverse rock record that spans from Archaean to Quaternary (Fig. 1C). Geologically, in the perspective of the North Atlantic, it represents the uplifted northwestern corner of the Barents Shelf. Svalbard's geological evolution is thus also studied as an analogue to the petroleum systems of the southwestern Barents Sea (e.g., Worsley 2008; Henriksen et al., 2011)

Tectonic setting

The western Barens Sea margin developed along the De Geer Zone megashear system during the opening of the Norwegian–Greenland Sea in Late Cretaceous to Paleogene times (Faleide et al., 2008). It can be subdivided into two large transform sections, the Senja Fracture Zone (SFZ) to the south and the WSM in the north (Fig. 1B). These transform segments are connected through the rifted Vestbakken Volcanic Province. The SFZ marks the westward extent of a basin province in which severely thinned continental crust is covered with up to 18–20 km of sedimentary strata. The WSM experienced transform tectonics followed by oblique rifting (Faleide et al., 2008). It comprises a sharply tapered necking domain where the crustal basement thins from more than 30 km to less than 10 km over a horizontal distance of approx. 100 km (Fig. 1D; sensu Peron-Pinvidic et al., 2013).

The evolution of the FG was strongly associated with the opening of the Norwegian–Greenland Sea. Breakup along the WSM connected the northeast Atlantic rift system with the rift system in the Arctic Ocean (Skogseid et al., 2000). The process can be divided into three stages:

1. Paleocene (before anomaly 24 / 53 Ma) – Pre–Eurekan stage:
The land bridge between Svalbard and North Greenland began to deform in Late Cretaceous time (88–80 Ma) as the opening of the Labrador Sea-Baffin Bay area advanced northwards (Døssing et al., 2013; Hosseinpour et al., 2013). Seafloor spreading commenced in Early Paleogene (anomaly 27, 61 Ma) and reached Baffin Bay between anomalies 24 and 25 (57–54 Ma). In this time interval, rifting in the Norwegian–Greenland Sea had reached its final stages and dextral wrench movements were ongoing along the De Geer Zone (Oakey & Chalmers, 2012).

2. Eocene (anomalies 24 – 13 / 53 – 34 Ma) – Eurekan stage:
Propagation of seafloor spreading into Baffin Bay and the onset of seafloor spreading in the Norwegian–Greenland Sea mark the start of this period. The movement of Greenland shifted to a

northwards direction, resulting in collision with both northeastern Canada and Svalbard, i.e. the Eurekan orogeny. As a consequence, the West Spitsbergen Fold-and-Thrust Belt (WSFB) formed on Svalbard. The sequence of events that led to the formation of the WSFB is a matter of active dispute. Braathen & Bergh (1999), Bergh et al. (2000), Faleide et al. (2008, 2015) and Leever et al. (2011) have argued that the structural geometries of the WSFB are best explained by strain partitioning of a single transpressional event. Tessensohn & Piepjohn (2000), CASE Team (2001) and Piepjohn et al. (2016), on the other hand, argued for two separate stages of deformation. In their view, a northwards movement of Greenland, lasting from anomaly 24 to 21, caused approximately orthogonal compression between Greenland and Svalbard. Then, in a second stage spanning from anomaly 21 to 13, Greenland moved NNW and introduced a dextral strike-slip motion along the De Geer Zone.

3. Oligocene – present (from anomaly 13 / 34 Ma) – Post–Eurekan stage:
This time interval is characterised by sustained seafloor spreading in the Norwegian–Greenland Sea and the Eurasian Basin and by cessation of spreading west of Greenland (Faleide et al., 2008, 2015). Along the conjugate Barents Sea–northeastern Greenland margins, dextral movements likely continued (Engen et al., 2008). In the Svalbard region, the tectonic regime probably shifted from dextral transpression or strike slip to transtension (Faleide et al., 2008, 2015, Piepjohn et al., 2016), and the formation of the Knipovich and Molloy ridges west of Svalbard.

The FG and the submerged Bellsund graben form a basin structure running along the west coast of Spitsbergen for about 150 km (Fig. 1A; Blinova et al., 2009). Structurally, Spitsbergen is dominated by three N–S-trending tectonic lineaments (Fig. 1A), namely the Hornsund, Billefjorden and Lomfjorden fault zones. These lineaments are long-lived and were active in a variety of tectonic settings (Fig. 1C; Myhre & Eldholm, 1988; Andresen et al., 1992; McCann & Dallmann, 1996). In the Cenozoic, the west coast of Spitsbergen was affected by thick-skinned deformation during the evolution of the WSFB and subsequent passive-margin formation (Fig. 2C; Bergh et al., 1997; Faleide et al., 2008).

The FG itself constitutes a half-graben to graben basin with steep basin-bounding normal faults cross-cutting the structures of the WSFB (i.e., Gabrielsen et al., 1992; Blinova et al., 2009). Structural style and thermal imprint within the basin differ significantly between the western and the eastern basin margins. In contrast to the rocks on Sarsøyra, the Paleogene sedimentary rocks on PKF, along the western margin of the FG (Fig. 2), exhibit depositional contacts to the basement in the footwall, compressional structures (Gabrielsen et al., 1992; von Gosen & Paech, 2001), a higher degree of lithification and a significantly higher thermal maturity (Fig. 3A, B). The difference in thermal maturity derived from compiled coal vitrinite reflectance data amounts to at least 85 °C (east = 107 °C for R_0 = 0.7, west = 192° for R_0 = 2.0, following Barker & Pawlewicz, 1994), corresponding to a minimum of 3.5 km in differential burial, assuming today's geothermal gradient of 24°C/km from the Sarstangen borehole (Betlem et al., 2018). The results of (U–Th)/He thermochronology by Barnes & Schneider (2018) also indicate a major difference in burial across the FG. They suggest that the PKF was exhumed later and substantially faster (>4 km since c. 34 Ma) compared with the west coast of Spitsbergen (2.5–3.5 km since c. 47 Ma).

These observations advance the exciting idea that the PKF was exhumed in association with a metamorphic core complex, as considered by Kleinspehn & Teyssier (1992). In a passive margin setting, metamorphic core complexes evolve due to rotation of deep-seated normal faults, forming low-angle detachments (e.g., Lister & Davis, 1989; Osmundsen & Péron-Pinvidic, 2018). In the context of the FG, considerable importance comes to the westerly-dipping crustal-scale Bouréefjellet Fault Zone (Schneider et al., 2018). It is located on the PKF, c. 18 km west of our field area in Sarsøyra (Fig. 2A), where the magnetic anomaly map indicates a slight shallowing of the basement beneath the FG (Fig. 3D). The Bouréefjellet Fault Zone juxtaposes the Mesoproterozoic amphibolite-facies Pinkiefjellet Unit against low-grade Neoproterozoic metapsammites (Hjelle et al., 1999; Dallmann et al., 2015). Schneider et al. (2018) further document highly dispersed Ar–Ar cooling ages across the Bouréefjellet Fault Zone, which date from 103 Ma to as late as 45 Ma within the Pinkiefjellet Unit.

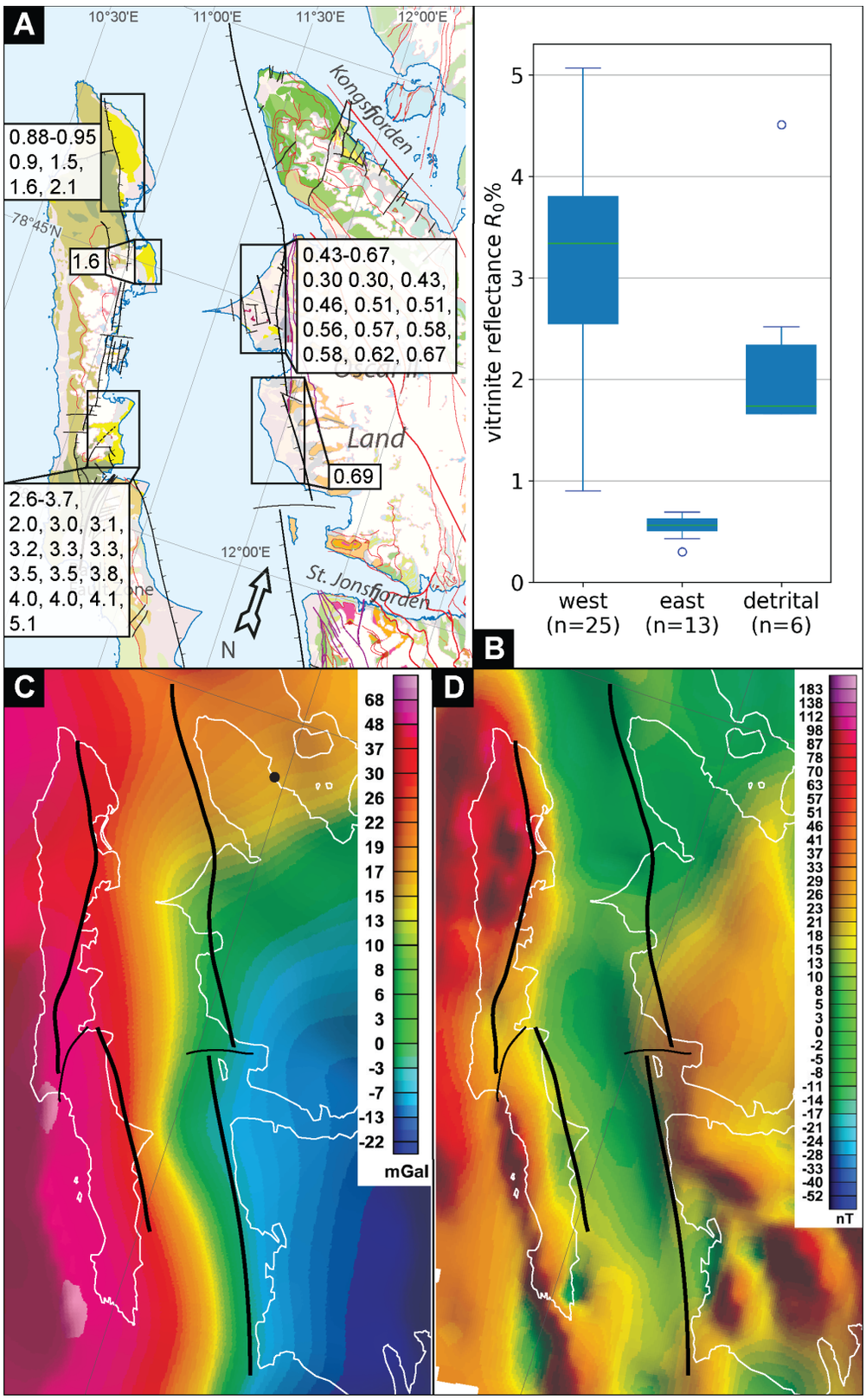

Figure 3. (A) Compilation of vitrinite reflectance values from literature (map from Dallmann et al, 2015, values from Rye-Larsen, 1982; Manum & Throndsen, 1986; Paech & Koch, 2001; Kleinspehn & Teyssier, 2016). (B) Statistical visualisation of the vitrinite reflectance data divided into coal fragments from the western and eastern basin margins as well as a detrital coal clast. Note that the coals along the western basin margin exhibit much higher vitrinite reflectance values than on the eastern side. The box-whisker plots indicate the minimum, lower quartile, average, upper quartile and maximum for the datasets. (C) Bouguer corrected gravity anomaly map exhibiting a decrease in crustal density from E to W (modified from Dallmann et al, 2015). (D) Magnetic anomaly map showing clear N–S-oriented features along the western margin of the FG. In the Sarsøyra area, an increase in magnetic susceptibility could indicate a slightly shallower basement level (modified from Dallmann et al, 2015). Magnetic and gravity data were collected and compiled by the Geological Survey of Norway.

Lithostratigraphy

The Central Basin hosts the majority of Cenozoic strata on Svalbard and formed as a foreland basin in association with the WSFB (Fig. 1A; Müller & Spielhagen, 1990; Jochmann et al., 2019; Helland-Hansen & Grundvåg, 2020). Along the west coast of Spitsbergen, four more outcrops of Paleogene rocks are known: Forlandsundet, Ny Ålesund, Renardodden and Øyrlandet (Fig. 1A; Dallmann et al., 2015). The relationships of these basin remnants to each other and to the Central Basin are uncertain.

The stratigraphy of the FG consists of continent-derived siliciclastics that make up the Buchananisen Group. It has been subdivided into eight units (Fig. 2B) of which six are exposed along the western and two along the eastern basin margin. The two units in the east are exposed on Sarsøyra and thus subjects of this study. Their classification has been inconsistent and calls for a thorough revision. Most authors acknowledge two Paleogene sedimentary units but name them differently. We use the formal names established by Dallmann et al. (1999), i.e. 'Sarsbukta conglomerate' for the older unit in the eastern part of the study area and 'Sarstangen conglomerate' for the younger unit exposed at Balanuspynten in the west (Fig. 4). They make up the Balanuspynten conglomerates which in turn are part of the Buchananisen Group (Dallmann et al., 1999).

Methods and data types

In this multidisciplinary study, we integrate various data types (Table 1), collected by us over a total of 38 field days on Sarsøyra in the summers of 2016, 2017 and 2018. Apart from the collection and analysis of sedimentological and structural data, an additional analytical program included K–Ar dating of a fault gouge, fission track thermochronology and palynostratigraphic dating of parts of the sedimentary succession. In addition, we had access to subsurface data, including 2D seismic profiles, acquired by Statoil in 1985 and SVALEX, i.e. University of Bergen, in 2001, as well as logs from the 7811/5–1 Sarstangen petroleum exploration well drilled by Norsk Polar Navigasjon AS in 1974 (Senger et al., 2019).

Field data

All orientation data were acquired with manual compasses and subsequently corrected for a magnetic declination of +7°. Orientation data are presented following the right-hand-rule, i.e. strike/dip. Visualisation of the structural and kinematic data was carried out with Stereonet (Allmendinger et al., 2013) and FaultKin software (Marrett & Allmendinger, 1990). Fold axes were calculated in Stereonet by applying the Bingham axial distribution algorithm to the respective bedding measurements.

Sedimentological logs were drawn in 1:50 scale, which allowed displaying layers down to 5 cm thickness. To determine the length of gaps due to unexposed parts of the sections we measured the distance directly or calculated it based on the horizontal distance between exposures and the prevailing dip. Scaled drawings and high-resolution photomosaics were obtained from well exposed outcrops.

XRD analysis and K–Ar dating

K–Ar low-temperature geochronology was used to date a clay sample from a fault gouge in the metamorphic basement. The formation of authigenic illite in fault gouges can be correlated with episodes of fault activity (Viola et al., 2016). The bulk clay-rich gouge was prepared for and dated by the K–Ar method at the Geological Survey of Norway (NGU), Trondheim, following procedures

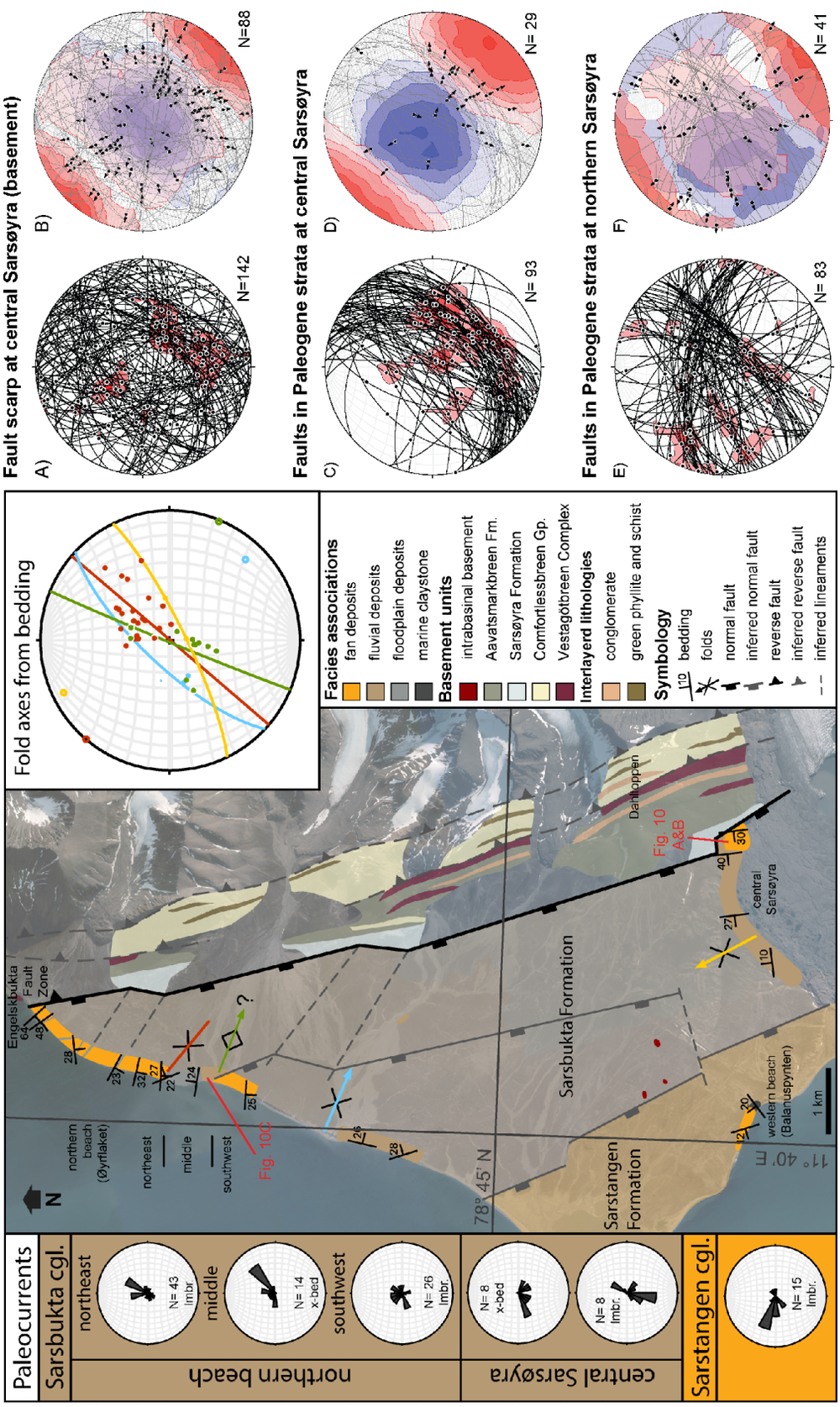

Figure 4. Field results from Sarsøyra. The map illustrates the extent of the geological units (transparent) and indicates the locations of the visited outcrops (solid). The outcrops are colour coded according to their lithofacies association. The stereoplot contains the bedding data (dots) that we used to reconstruct the orientation of fold axes (lines and circles). The location of the map is marked in Fig. 2. The map includes data from Hjelle et al. (1999) and Krasilscikov et al. (1995). Paleocurrent data indicate preferential northward flow for the northern outcrops and southwestward flow for the central exposures of the Sarsbukta conglomerate. In the Sarstangen conglomerate, westward flow prevailed. The kinematic data from fault planes suggest a consistent NW–SE extension trend throughout the study area in the basement (B) as well as in the Paleogene basin fill (D and F). The left stereoplots (A, C and E) display all the fault data collected while the right stereoplots (B, D and F) only include data with clear kinematic indicators. From the clear kinematic data points, the tension-axes (red contours in B, D and F) were determined.

Table 1. Summary of the data collected and utilised for this study.

Data type	Number	Application	Source
Field data			
Fault and kinematic measurements	~450	Reconstruction of stress axes	this study
intraclast fractures	~50	Reconstruction of maximum elongation	this study
Bedding measurements	50	Construction of fold axes	this study
Paleocurrent indicators	114	Paleocurrent directions	this study
Sedimentary logs	370 m	Description of the sedimentary succession	this study
Scale drawings	5	Assessment of sedimentary architecture	this study
Photographs	1000s	Documentation of outcrops	this study
Geochronology			
K–Ar dating	1	Growth of illite in a fault gouge	this study
X-ray diffraction (XRD)	1	Mineral composition, authigenic clay in a fault gouge	this study
Apatite and zircon fission track	5	Cooling ages of basement and sedimentary rocks	this study
Palynology	10	Age of sedimentary deposits	this study
Subsurface			
Composite well log from 7811/5–1 Sarstangen petroleum exploration well	1	Depth of basement	Senger et al. (2019)
Gravimetry	1	Density and isostatic state of the crust	Geological Survey of Norway
Magnetics	1	Depth of basement and location of lineaments	Geological Survey of Norway
Literature			
Vitrinite reflectance	44	Thermal evolution of the basin fill	see Fig. 3

described in Viola et al. (2018). Five clay particle size fractions (<0.1 µm, 0.1–0.4 µm, 0.4–2 µm, 2-6 µm and 6–10 µm) were generated and collected using a combination of stokes settling and continuous flow centrifugation. Radiogenic $^{40}Ar^*$ concentrations were measured by isotope dilution on an IsotopX NGX multicollector noble gas mass spectrometer using a pure ^{38}Ar spike (Schumacher, 1975). Potassium concentrations were determined by fluxing ~50mg of sample material in $Li_2B_4O_7$ and dissolving the resulting glass bed in HNO_3, which was then analysed using a Perkin Elmer 4300 DV ICP–OES. Ages were calculated using the decay constants of Steiger & Jäger (1977).

All samples were analysed by XRD at the laboratory of the NGU. Details of instrument and measurement parameters are given in Supplement Material 1 of Scheiber et al. (2019). The purpose of the XRD analyses was to determine the mineralogical composition of the fault gouge sample and to identify newly formed clay minerals, i.e. illite (Schönenberger et al., 2019).

Fission track thermochronology

Low-temperature dating is now regularly employed to recover cooling histories of geological field areas. Because samples from previous apatite and zircon fission track (AFT and ZFT) studies are too widely spaced to address potential structural offsets (Blythe & Kleinspehn, 1998; Dörr et al., 2012), we conducted a pilot study in the St. Jonsfjorden – PKF region in 2016. Five samples were collected along a horizontal transect between the innermost portion of St. Jonsfjorden and the sedimentary basin on PKF (Fig. 2A). The study was designed to investigate whether the substantial differences in cooling history across the Forlandsundet could be attributed to brittle faulting, and if so, to impose temporal constraints. In this paper, we briefly discuss the results from two samples considered to be representative of the AFT dataset.

Palynology

Palynology can be used for the determination of the stratigraphic age of sedimentary rocks based on the analysis of pollen, spores and algae (palynomorphs). The palynomorphs themselves, as well as their distribution and abundance, change rapidly over time due to biological evolution and the composition of the paleovegetation. Thus, characteristic palynomorph assemblages can be assigned to certain geological times and regions (Traverse, 2007). Fine-grained sandstones and siltstones, as well as coal, were sampled for this method. Ten samples were analysed by the laboratory of the Institute for Applied Geosciences at the University of Darmstadt in Germany following standard procedures as described by Kaiser & Ashraf (1974). These include the treatment of the samples with hydrochloric acid (HCl), hydrofluoric acid (HF) and potassium hydroxide (KOH). Flocculating organic matter was removed and the transparency of palynomorphs improved by briefly oxidising the residue with hydrogen peroxide (H_2O_2) after sieving with a mesh size of 10 µm.

The eastern Forlandsundet Graben

In the following, we present our results in geochronological order, starting with a brief description of the basement units, followed by our presentation of data from the Paleogene basin infill. Fig. 4 summarises the most important newly acquired field data.

Basement units along the eastern boundary of the Forlandsundet Graben

The tectono-stratigraphy of the basement along the eastern basin margin comprises metasedimentary lithologies that are parallel-layered and dip towards the WNW (Fig. 4). The most complete succession is exposed in central Sarsøyra where evidence of brittle deformation is largely absent. The actual contact between the basin fill and the basement is not exposed in the field area, but the distance between basement outcrops and the Paleogene sedimentary rocks is small, usually on the order of metres to tens of metres. Seven lithological units in the metamorphic basement were distinguished in the field and are presented briefly from the basin boundary eastwards into the footwall (Fig. 5):

1. **Light grey marble** of the Sarsøyra Formation, part of the Upper Ordovician to Middle Silurian Bullbreen Group, makes up the degraded fault scarp of the Paleogene basin in central Sarsøyra where it

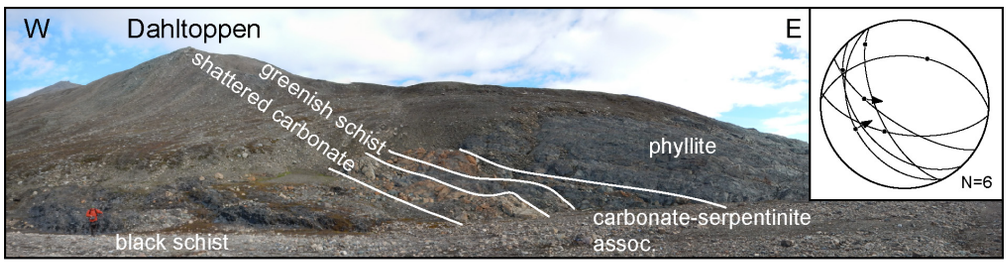

Figure 5. Annotated photograph showing the tectono-stratigraphy of basement units in central Sarsøyra (Fig. 4). Two additional units that are exposed are not included in the picture but described in the text; a light grey marble that hosts the contact to the Paleogene strata and a quartzite to the west and east, respectively. Upper right: Stereonet representation of fault planes (lines), striations (poles) and kinematics (arrows) in the basement section. Location: N 78.7251°, E 11.9041°.

has a thickness of several hundred metres (Fig. 4; Hjelle et al., 1999). Outcrops of the marbles in central Sarsøyra hold abundant fault planes with clear kinematic indicators such as striae, steps and mineral fibres. Several larger outcrops of the Sarsøyra Formation are located along the eastern basin boundary (Fig. 4). However, the unit is missing in the coastal outcrop at the northern beach (Fig. 6). A small patch of light grey marble is exposed in the riverbed behind the outcrop shown in Fig. 6. Therefore, a thin sliver of the Sarsøyra Formation is preserved between the basin and the other basement units in the north. In the beach cliff it is eroded by a recent river mouth. The thickness of the Sarsøyra Formation must decrease towards the north as the distance between the first basement units shown in Fig. 6 and the Paleogene basin fill is only around 50 m. A likely explanation is that the Sarsøyra Formation is progressively excised along the tectonic contact to the Paleogene basin.

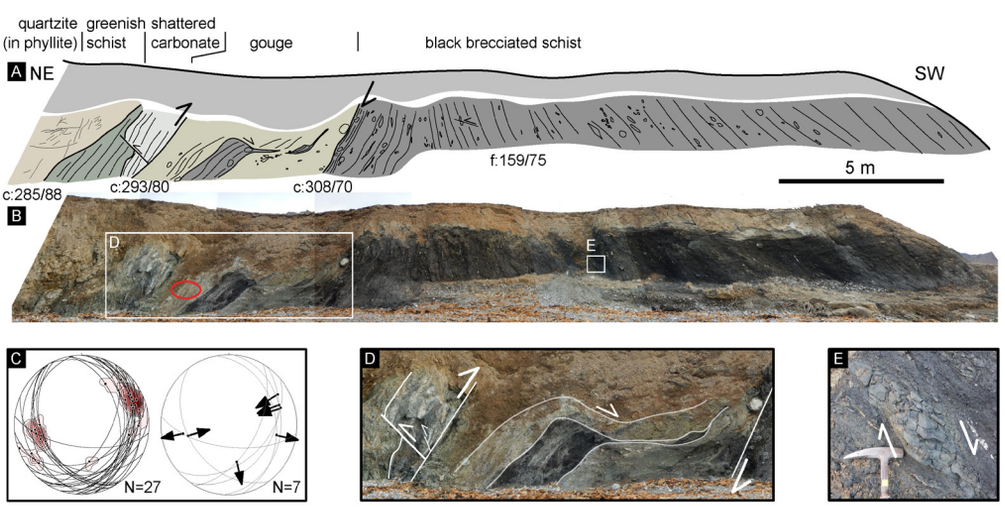

Figure 6. (A) Line drawing of the Engelskbukta Fault Zone in proximity to the basin fill on northern Sarsøyra based on a photomosaic (B) and field observations (location: N 78.8103°, E 11.7269°). The fault zone incorporates heavily brecciated rocks of the same lithological units exposed in central Sarsøyra (Fig. 5). Red ellipse marks the area where the gouge sample (20170810–5) for K–Ar dating was taken. Note that the outcrop is oriented NE–SW. Structural measurements are annotated in the drawing (A); c – contact, f – foliation. C) Left: Stereonet representation of fault planes (lines) with striations (poles) from the hanging wall (NE of the gouge) of the Engelskbukta Fault Zone. Right: Fault planes (lines) with kinematics (arrows). The data are dominated by NNW–SSE-striking conjugate faults. The kinematics suggest oblique reverse movement. D) Close-up of a ~6 m-wide fault gouge that shows shear-band like smearing of a black lens indicating reverse movement on the main fault. Smaller antithetic reverse faults that splay off the gouge support this interpretation. E) Towards the southwest, sigmoidal-shaped carbonate lenses suggest normal movement closer to the basin boundary.

2. Thinly foliated **black schist** containing discontinuous quartzite lenses. It exhibits tight, cm-scale folding in a few places and is otherwise dominated by a planar foliation, oriented 326/80. Patches with a rusty weathering colour occur and indicate that the lithology contains iron-rich minerals. This unit is assigned to the Aavatsmarkbreen Formation which is also part of the Upper Ordovician to Middle Silurian Bullbreen Group (Hjelle et al., 1999). It makes up 27 m in the central Sarsøyra outcrop (Fig. 5). In the north, this unit is heavily brecciated and a cataclastic foliation has been superimposed over the older ductile fabric (Fig. 6).

3. Light grey **shattered carbonate**, probably silica-cemented, as it is very hard and brittle. We consider it to be part of the Aavatsmarkbreen Formation (Upper Ordovician to Middle Silurian Bullbreen Group). It is 4 m wide in the outcrop in central Sarsøyra (Fig. 5). At the northern beach, the unit is cut by a gouge zone and only a 1.5 m-wide sliver is exposed (Fig. 6).

4. Well foliated **greenish schist** containing chlorite, reddish mineral alterations and quartz veins. The unit comprises pyrite nodules up to 5 mm in diameter and weathers light brown. It is probably part of the Aavatsmarkbreen Formation (Upper Ordovician to Middle Silurian Bullbreen Group) and spans over 6 m in the central Sarsøyra outcrop (Fig. 5). In the northern beach section, this unit comprises only a 1.5 m-wide sliver that was affected by reverse thrusting in the adjacent unit (Fig. 6).

5. **Carbonate-serpentinite association** that we consider to be part of the Neoproterozoic Vestgötabreen Complex (Kanat & Morris, 1988; Hjelle et al., 1999). In the outcrop at the central Sarsøyra locality it is 4 m wide, while it is absent in the outcrop at the northern beach (Fig. 6).

6. Grey **phyllite** that covers an outcrop width of several tens to hundreds of metres in central Sarsøyra (Figs. 4 & 5). The grey phyllite is the characteristic lithology of the Aavatmarkbreen Formation and accounts for most of its thickness. It is well foliated and can be interlayered with conglomerates, quartzites and marbles (Kanat & Morris, 1988; Hjelle et al., 1999). In the eastward continuation of the outcrop at the northern beach, quartzites and schists with localised zones of high strain define the exposure. These rocks could belong to either the Aavatmarkbreen Formation or the Comfortlessbreen Group (see below).

7. A several hundred meters-thick **quartzite** unit crops out farthest to the east in central Sarsøyra (Fig. 4). The quartzites represent the upper part of the Vendian Comfortlessbreen Group (Kanat & Morris, 1988; Hjelle et al., 1999).

AFT and ZFT thermochronology

We obtained AFT and ZFT data from samples of metagabbroic and metasedimentary rocks collected in St. Jonsfjorden and on PKF (Fig. 2A). However, the quality of the measurements varies, mainly due to a low number of countable tracks or grains. The age and length data presented here do not represent single unique thermal events. Thermal modelling would be required to extract a best-fit thermal history from the individual age/length pairs. Given the poor quality of the recovered data, we have little faith that modelling would provide meaningful geological constraints. Therefore, our interpretation of the data will be limited to some key observations.

The ZFT ages from PKF (Electronic Supplement 1) all pre-date the proposed timing of the basin formation by far and suggest that the Paleogene sedimentary succession did not experience temperatures above ~240 °C (Gallagher et al., 1998; Bernet, 2005). We consider this maximum temperature to represent an additional boundary condition to confine the time-temperature model proposed by Barnes & Schneider (2018) (Fig. 7).

Two AFT ages from PKF, KKF–11 and KKF–18 (both Paleogene sandstones), exhibit acceptable results (Electronic Supplement 2). The short mean track lengths indicate that the rocks were reheated or have resided in the apatite partial annealing zone (APAZ; 60 to 100 °C; Gallagher et al., 1998) for an extended period during the latest exhumation event (Fig. 7). Cooling rates may have been slightly lower than those proposed by Barnes & Schneider (2018), and the plateau they indicated could perhaps be moved into the APAZ (Fig. 7). However, due to weak statistics of the two KKF samples, this is a poorly constrained interpretation. Sample KKF–04 (Paleogene sandstone) was disregarded because too few tracks were measured to justify a geological interpretation.

Sample SJ–05 (metagabbro) from St. Jonsfjorden contained a sufficient number of measured grains and tracks to deliver a statistically viable age (Fig. 7). Since the sample was taken from a metagabbro, any inherited thermal history can be neglected. The relatively short mean track length (also true for SJ–07) indicates slow cooling. Taken by itself, the 'apparent age' is in conflict with the time-temperature data and model for Oscar II Land proposed by Barnes & Schneider (2018) who suggest tempertures well above the APAZ (Fig. 7). Many factors could have caused this discrepancy – one of them is that an AFT apparent age does not by itself reflect a unique position on the time-temperature path. The most obvious problem, however, is that sample SJ–05 was collected 14 km inland from the Paleogene basin and over 6 km inland from the closest sample collected by Barnes & Schneider (2018). In between, several structures related to the WSFB cut the succession and possibly juxtaposed rocks with different thermal histories. With no other samples analysed from localities in closer vicinity to the basin or the sample sites of Barnes & Schneider (2018) our spatial control is low, which prevents a sound geological interpretation of the AFT data. For sample SJ–07 (metagabbro), we neglect a geological interpretation because the associated uncertainties are too high.

These findings imply that the Paleogene sedimentary rocks on the eastern and the western sides of the basin reflect different stages in the overall basin evolution. Barnes & Schneider (2018) suggested that the western margin of the FG was buried and exhumed along with the basement of PKF (see also Schneider et al., 2018). Our results are consistent with the general interpretation of Barnes & Schneider (2018) and support a difference in thermal history laterally across the FG.

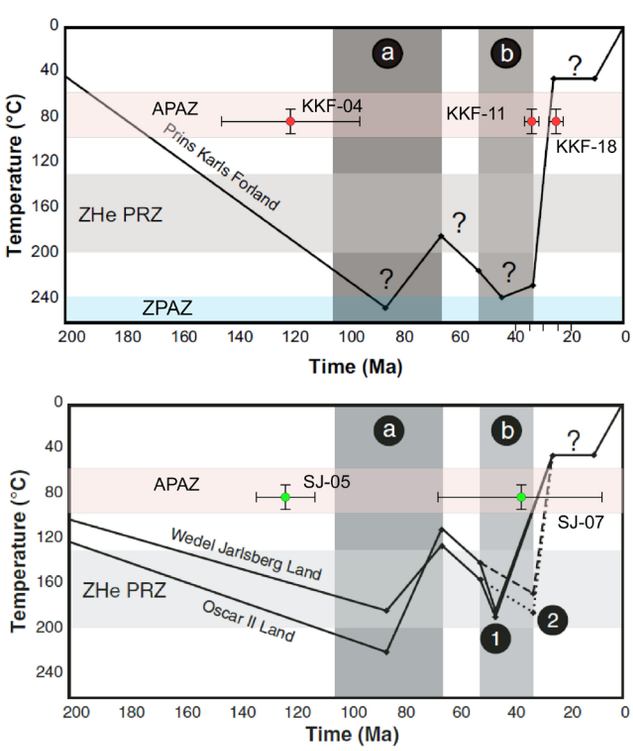

Figure 7. Schematic time-temperature model (ZHe) by Barnes & Schneider (2018) with red and green dots marking our AFT ages (error bars indicating the 95% certainty intervals). The model suggests that PKF experienced higher temperatures for longer, and subsequently experienced faster uplift than Oscar II Land. For the Eurekan orogeny (b), two cases were modelled for each locality. Oskar II Land (solid line): max. 185 °C at 47 Ma cooling to 20 °C at 30 Ma. Oskar II Land (dashed line): max. 175 °C at 34 Ma cooling to 20 °C at 32 Ma. PKF: max. >200 °C cooling to ~45 °C at 26 Ma. The figure is modified from Barnes & Schneider (2018).

Basement-basin contact: the Engelskbukta Fault Zone

In northern Sarsøyra, the basement units in proximity to the Paleogene basin fill are heavily deformed. Despite that, the tectono-stratigraphy (Fig. 6A, B) appears to be the same as in central Sarsøyra (Fig. 5). The most prominent features are a c. 6 m-wide fault gouge and a 20 m-broad zone of black schist showing westward-increasing amounts of cataclasis and brecciation. The fault gouge separates the black brecciated schist from the lithologies to the east. Within the gouge, a schist lens is smeared out in a shear-band-boudin-like manner (Fig. 6B). The formation of shear-band boudins is associated with synthetic drag in shear zones (Goscombe & Passchier, 2002; Passchier & Trouw, 2005). Therefore, we interpret this structure to indicate top-to-the-west reverse kinematics. This interpretation is supported by the smaller antithetic reverse faults that splay off the gouge into the surrounding rocks (Fig. 6C, D). Structural measurements in the hanging wall (Fig. 6C) also show a NNW–SSE-striking set of conjugated faults with reverse-sense kinematics. The foliation within the black brecciated schist changes its orientation eastwards, i.e., towards the basin. At the contact to the gouge, a 20 cm-wide zone is tightly folded on cm-scale and southwestwards the foliation is dipping steeply to the northeast (Fig. 6A). Within two metres distance from the contact, the foliation starts dipping steeply to the WSW and gradually shallows (Fig. 6A). Lenses within the unit show sigmoidal geometries (Fig. 6E) and suggest top-to-the-west normal movement. We attribute these features to the basin-bounding fault which must be located in close proximity because Paleogene exposures can be found 50 m southwest of the outcrop.

XRD analyses and dating of illite in a fault gouge

We sampled the fault gouge to conduct XRD analysis and K–Ar dating of illite (sample 20170810–5; Fig. 6B). All grain-size fractions consist mainly of chlorite, chlorite-smectite mixed-layer and illite/muscovite. Due to the lack of structural data for mixed-layer clays, only semi-quantitative mineral concentrations could be acquired (Table 2). The coarsest fractions (6–10 µm, 2–6 µm and 0.4–2 µm) show decreasing intensities of the typical 2M1 polytype peak with decreasing grain-size fractions, and furthermore comprise minor amounts of epidote, talc, zeolite and possibly rutile. The finest grain-size fractions have no 2M1 illite.

A measure for the illite crystallinity can be represented by the Kübler Index (KI; Kübler, 1967), i.e. the full width at half maximum (FWHM) of the major 10 Å (001) illite/muscovite peak. In the studied samples, KI increases with decreasing grain size suggesting an increase of diagenetic illite over detrital illite/muscovite.

Table 2. Mineralogical composition of different grain-size fractions of sample 20170810–5 (location: N 78.8103°, E 11.7269°). Due to the lack of structural data for mixed–layer clays, quantification [wt%] could only be performed in a semi-quantitative way. Mineral abbreviations are: chl = chlorite, chl–sm mixed-layer, ill/musc = illite and/or muscovite, epi = epidote, tlc/zeo = talc and/or zeolite, rt = rutile

fraction [µm]	chl	chl–sm	ill/musc	epi	tlc / zeo	rt	illite crystallinity [$\Delta^{\theta}2q$]
<0.1	mineral quantification is limited due to poor crystallinity; identified minerals are: chl, chl-sm and ill/musc						0.58
0.1–0.4	15–30	15–30	>30				0.47
0.4–2	15–31	5–15	>30	<5	<5	<5	0.24
2–6	15–32	5–15	>30	<5	<5	<5	0.18
6–10	15–33	5–15	>30	<5	<5	<5	0.16

The K–Ar dating results of the fault gouge (Fig. 6C) are presented in Table 3. The finest recoverable grain-size fraction (<0.1 µm) is generally considered to be dominated by authigenic illite formed during the most recent faulting event (Viola et al., 2016 and references therein). As the two finest fractions comprise both 1M illite and illite-smectite mixed-layer clays, but no 2M1 illite, both of these fractions contain only authigenic K–bearing minerals. Therefore, we interpret the 53.5 ± 1.0 Ma age to represent a faulting event. The 83.0 ± 1.3 Ma age of the <0.4 µm fraction is a mixed age of purely authigenic minerals, suggesting that faulting occurred already some time before ~83 Ma. For the coarser grain fractions, our dataset precludes a geological interpretation without further sampling and analysis.

Table 3. Summary of the K–Ar dating of different grain fractions in the fault gouge sample 20170810–5 (location: N 78.8103°, E 11.7269°). We interpret the 53.5 and the 83.0 Ma ages as related to fault activity.

Sample	Grain size fraction (µm)	K (%)	Rad. ^{40}Ar (mol/g)	Rad. ^{40}Ar (%)	Age (Ma)	Error (Ma)
Sarsøyra	<0.1	1.617	1.5220E–10	25.4	53.5	±1.0
Sarsøyra	0.1–0.4	3.078	4.5351E–10	58.4	83.0	±1.3
Sarsøyra	0.4–2	3.539	9.11667E–10	84.1	142.7	±2.1
Sarsøyra	2–6	3.504	1.59532E–09	97.0	245.1	±3.6
Sarsøyra	6–10	3.396	1.80656E–09	98	283.3	±4.4

We name this structure the Engelskbukta Fault Zone (Fig. 4) and interpret the gouge-bearing parts of it as a back thrust within the WSFB. For that, our main arguments are the top-to-the-west reverse kinematics (Fig. 6) and the K–Ar age of 53.5 ± 1.0 Ma for illite growth. The age coincides with the final break-up at the Norwegian continental margin (55–54 Ma; Faleide et al., 2008) which in turn drove the formation of the WSFB. The Engelskbukta Fault Zone probably represents a continuation of the Svartfjella, Eidembukta and Daumannsodden lineament (SEDL; Fig. 2A) described by Maher et al. (1997). The SEDL constitutes a major orogen-parallel lineament of the WSFB in the area south of St. Jonsfjorden with a complex and long-lived kinematic history (Maher et al., 1997). However, for the Engelskbukta Fault Zone our data only show clear evidence for back thrusting and an indication of normal movement. Considering a link between the Engelskbukta Fault Zone and the SEDL, we have documented and dated activity on a long-lived regional structure. The lineament runs along much of Spitsbergen's west coast and is everywhere in the footwall of the normal fault bounding the FG.

Paleogene fill of the eastern Forlandsundet Graben

The stratigraphy exposed on Sarsøyra was described briefly by previous authors (Rye-Larsen, 1982; Kesper, 1986; Sperling, 1990; Gabrielsen et al., 1992; Dallmann et al., 1999; Kleinspehn & Teyssier, 2016). Below, we document the sedimentary units in more detail and describe their depositional environments on the basis of lithofacies (c.f., Miall, 1977a, 1985) and lithofacies associations, as summarised in Tables 4 & 5. Our interpretation is aided by fossils that occur in abundance in some of the sedimentary rocks.

Sedimentology of the Sarsbukta conglomerate (?Late Eocene?)

The sedimentary units of the Sarsbukta conglomerate were divided into eleven lithofacies (Electronic Supplement 3). We distinguish three distinct depositional elements within the Sarsbukta conglomerate (Table 4).

Table 4. Summary of lithofacies associations recognised in the Sarsbukta conglomerate. See Electronic Supplement 3 for lithofacies descriptions.

Lithofacies association	Lithofacies code	Interpretation
Alluvial fan	Gm, Gp, Sm, P, C	Debris and high-energy stream flow deposits on alluvial fans
Fluvial	Sm, St, Sp, Sh, Sr, Gp, P, C, Gm	Deposition by sineous fluvial channels with bar formation
Floodplain	Fl, S, P, C	Floodplain and overbank deposits

Table 5. Summary of lithofacies associations recognised in the Sarstangen conglomerate. See Electronic Supplement 5 for lithofacies descriptions.

Lithofacies association	Lithofacies code	Interpretation
Fan	B	Mass-flow deposits on a fan
Fluvio to deltaic	Gm, St	Fluvial to deltaic or coastal system
Marine offshore deposit	M	Distal fan-delta or basin-floor deposit

Lithofacies association A: Alluvial fan and proximal stream

Description - Lithofacies association A contains thick successions of massive gravel with thinner beds of planar cross-bedded gravel, massive sandstone and fines as subordinate lithologies (Table 4 & Fig. 8). Paleosols (Fig. 8C), as well as coal (Fig. 8E), are present in interbedded finer-grained deposits. The conglomerates are coarse with clasts of pebble to cobble size and poorly sorted (Fig. 8A). Most of the beds are massive. Some beds exhibit sedimentary structures like horizontal stratification, planar cross-bedding (Fig. 8D) and clast imbrication. The bases of massive gravel beds are commonly erosive while the sandstones overlie the conglomerates conformably. Lithofacies association A is exposed in central Sarsøyra and along the northeastern part of the northern beach (Fig. 4). At the northern beach, this lithofacies association interfingers with finer-grained deposits (Figs. 4 & 9).

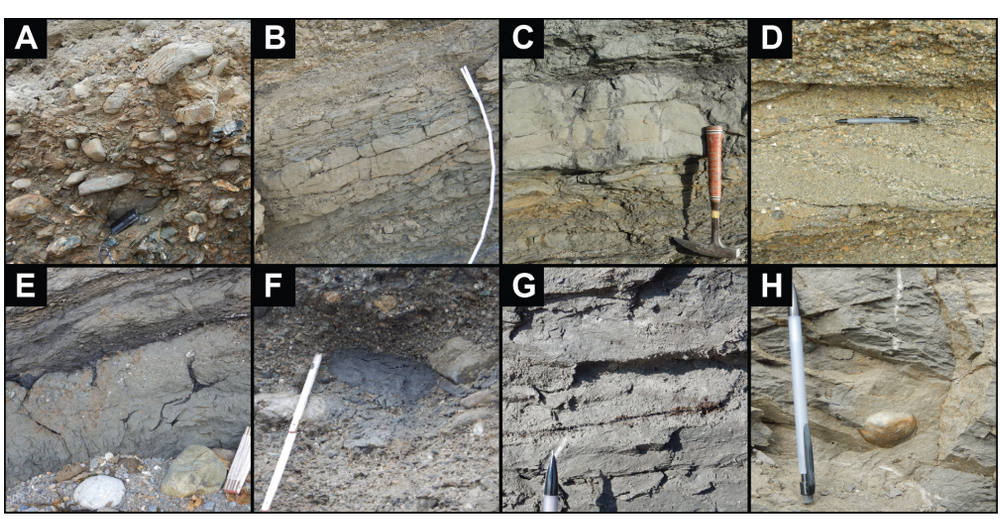

Figure 8. Close-up photographs of lithofacies in the Sarsbukta conglomerate (A–E; Electronic Supplement 3) and the Sarstangen conglomerate (F–H; Electronic Supplement 5). (A) Massive gravel. (B) Massive sandstone. (C) Massive sandstone with rootlets that originate from the paleosol above. (D) Planar cross-bedded very coarse sandstone. (E) Coal bodies embedded in fines. (F) Angular mud clast in massive gravel of the Sarstangen conglomerate. (G) Coal streak in trough cross-bedded very fine sandstone. (H) Well-rounded pebble, possibly a dropstone, in the marine claystone.

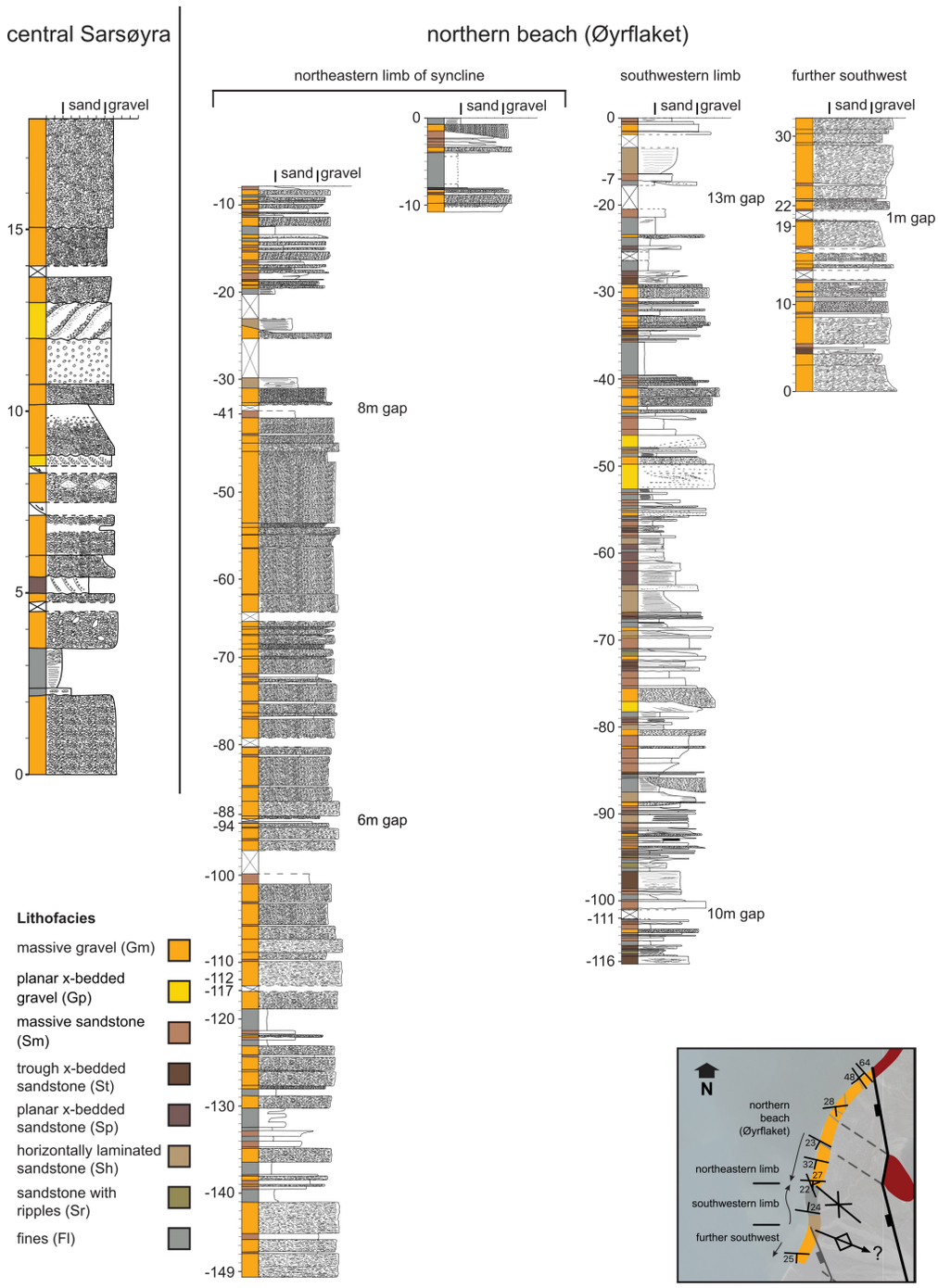

Figure 9. Sedimentary logs recorded by us in central Sarsøyra (left; Fig. 10B) at the northern beach (right). The logs at the northern beach are levelled (0 m) to the centre of the syncline (inset map, see Fig. 4 for location). Vertical scale is labelled with negative values to indicate that the logs are levelled to the top-horizon in the centre of the syncline. The arrows on the inset map point towards the stratigraphic upside. See Electronic Supplement 3 for detailed description of the lithofacies. Uncompressed logs in 1:50 scale are provided in Electronic Supplement 4.

Interpretation – Lithofacies association A represents deposition on an alluvial fan. The presence of poorly sorted conglomeratic beds with inverse grading suggests that mass flow events, particularly debris flows, occurred (Blair & McPherson, 1994). A fluvial influence is manifested by sandy deposits, clast imbrication and high-angle cross beds. In central Sarsøyra, the general sediment transport direction is towards the west (Fig. 4), i.e., away from the basin-bounding fault. Fig. 10A illustrates an exposure in central Sarsøyra that contains downlap of planar cross-bedded gravels and sandstones onto a conglomerate body. We interpret these structures to represent downstream sediment progradation, possibly associated with

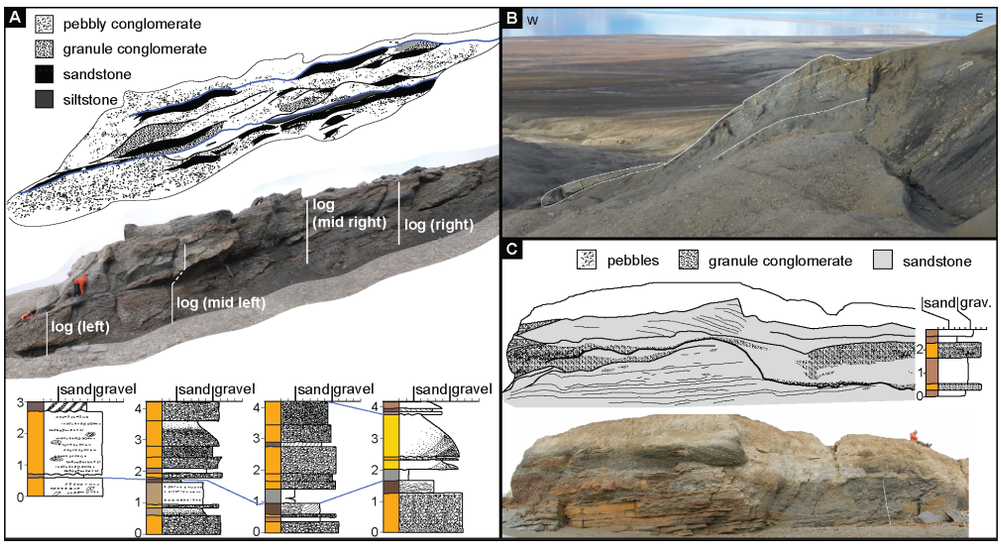

Figure 10. Detailed assessment of sedimentary structures in outcrops in central Sarsøyra (A–B) and at the northern beach (C). See Fig. 9 for the legend of the logs and Fig. 4 for location.

an extensional monocline that covered the fault scarp during deposition (Fig. 10B). The presence of paleosols indicates that parts of the fan experienced longer periods of inactivity.

Lithofacies association B: Fluvial channels

Description - Lithofacies association B is dominated by sandstones that are massive, trough or planar cross-bedded, horizontally laminated or contain ripples but also includes massive and planar cross-bedded gravels with clast size pebble and smaller (Table 4 & Fig. 8). Bed thickness varies from 5 cm to approximately 1 m. Planar (Fig. 8D) and trough cross-bedding are the most important sedimentary structures. Leaf imprints, coal, rootlets and paleosols are abundant. The lithofacies association is exposed in central Sarsøyra, along the northern beach and in a small river cut between those localities (Fig. 4).

At the northern beach, the sedimentary architecture is well exposed in headland sections. Fig. 10C presents a channel that cuts into a horizontally laminated and partly planar cross-bedded, fine-grained sandstone. The channel fill consists of pebbles at the base grading into granule conglomerates and massive as well as planar cross-bedded sandstones. Pebble horizons and granule bodies occur in the sandstone. A thick, planar cross-bedded sandstone overlies the succession.

Interpretation – The common occurrence of coals, paleosols, rootlets and apparent lack of marine fossils in lithofacies association B indicates a continental environment. Trough and planar cross-beds in the sandy units suggest migrating 2D and 3D dunes under unidirectional flow in a fluvial system. Together with erosive channel bases such as the one illustrated in Fig. 10C, the sedimentary structures indicate that lithofacies association B represents fluvial channel deposits. Cannibalisation and amalgamation of channel bodies as seen at the northern beach (Fig. 10C) are typical features of braided river deposition (Rust, 1972; Miall, 1977b). The high-angle planar cross-beds in the top layer (Fig. 10C) are attributed to lateral accretion of a lingoid bar as the cross-beds are oriented sub-parallel to the channel trend and thus to the flow direction (Campion et al., 2000). This mode of deposition requires at least seasonal bar-top flow and therefore develops preferentially in fluvial systems with high variations in discharge. We interpret the pinching interlayered granule and sand structures (Fig. 10C, upper left) to represent trough cross-stratification deposited by dunes along the bar flanks. The up to 4 m-thick intervals of very fine-grained sediments indicate that substantial floodplain (see below) sediments were accumulated and lead to the conclusion that the fluvial channels had a rather high sinuosity. Thus, in the

apparent absence of lateral accretion (point bar) deposits, we interpret lithofacies association B to represent a braided river with relatively high sinuosity.

Lithofacies association C: Floodplain sediments

Description - Lithofacies association C consists of fines with subordinate sandstones (Table 4). The silt to clay intervals reach thicknesses of several metres, while sandstone thicknesses do not exceed 50 cm (Fig. 9). The deposits are horizontally laminated but sometimes contain cm-scale current ripple lamination. Coal stringers and larger coal fragments are common in this lithofacies association. It is exposed in the middle section of the northern beach (Fig. 9) and interfingers with the fan deposits towards the northeast (Figs. 4 & 9).

Interpretation - Coal stringers and fragments are strong arguments for a terrestrial deposition of lithofacies association C. The fine grain size and horizontal lamination indicate sedimentation from suspension and, thus, a low-energy transport mechanism. However, the occasional ripples represent episodes of unidirectional flow. We interpret them as overbank deposits that formed during flood events. The thickness of the overbank deposits is significantly lower than the thickness of sediments deposited in channels and bars (Fig. 9). This relationship most likely reflects the common erosion of fine-grained lithofacies by high-energy currents in the braided river environment (Nanson & Croke, 1992). Thus, this lithofacies association is generally only preserved as a thin and discontinuous layer. The logs in Fig. 9 show this characteristic feature in many places but also contain thicker intervals that support our interpretation of a sinuous (braided) river that allowed the establishment of extensive floodplains.

Sedimentology of the Sarstangen conglomerate (Oligocene)

The sedimentary units of the Sarstangen conglomerate were divided into three lithofacies (Electronic Supplement 5). We distinguish three depositional elements within the Sarstangen conglomerate (Table 5).

Lithofacies association A: Alluvial fan / Fan delta (?)

Description - Lithofacies association A is entirely made up by the sedimentary breccia (Table 5) and exhibits an erosive contact to the underlying sediments. It consists of chaotic (Fig. 11) as well as stratified conglomerate beds containing large angular outsize boulders (Fig. 12).

Interpretation - The most striking feature in this lithofacies association are angular boulders with a diameter of up to 4 m (Fig. 12). We consider that the boulders were deposited by rockfalls onto a fan. Because the angularity decreases for smaller clasts and a sandy matrix is present, rockslides and avalanches probably had little importance as they produce angular detritus across all grain sizes (Blair & McPherson, 1994). Steep topography is required for rockfall deposition and was likely generated by the offset of an intrabasinal fault. The existence of a major structural feature in proximity to Balanuspynten is suggested by magnetic anomalies (Fig. 4, Krasilscikov et al., 1995) as well as the difference in the top basement level between central Sarsøyra (sea level; Fig. 4) and the 7811//5–1 petroleum exploration well 5 km (Fig. 2A) to the west on the Sarstangen spit (1046 m depth; Senger et al., 2019; a lithological log is provided in Electronic Supplement 6).

As for the fan itself, the well-developed stratification of dm–thick, poorly sorted and clast-supported conglomerate beds (Fig. 12) suggests deposition in couplets by sheetfloods. However, the layer dip of 12° to 17° is too steep for a sheetflood dominated fan (Blair & McPherson, 1994) and promotes a rotation subsequent to deposition or alternative depositional modes, e.g., debris flows.

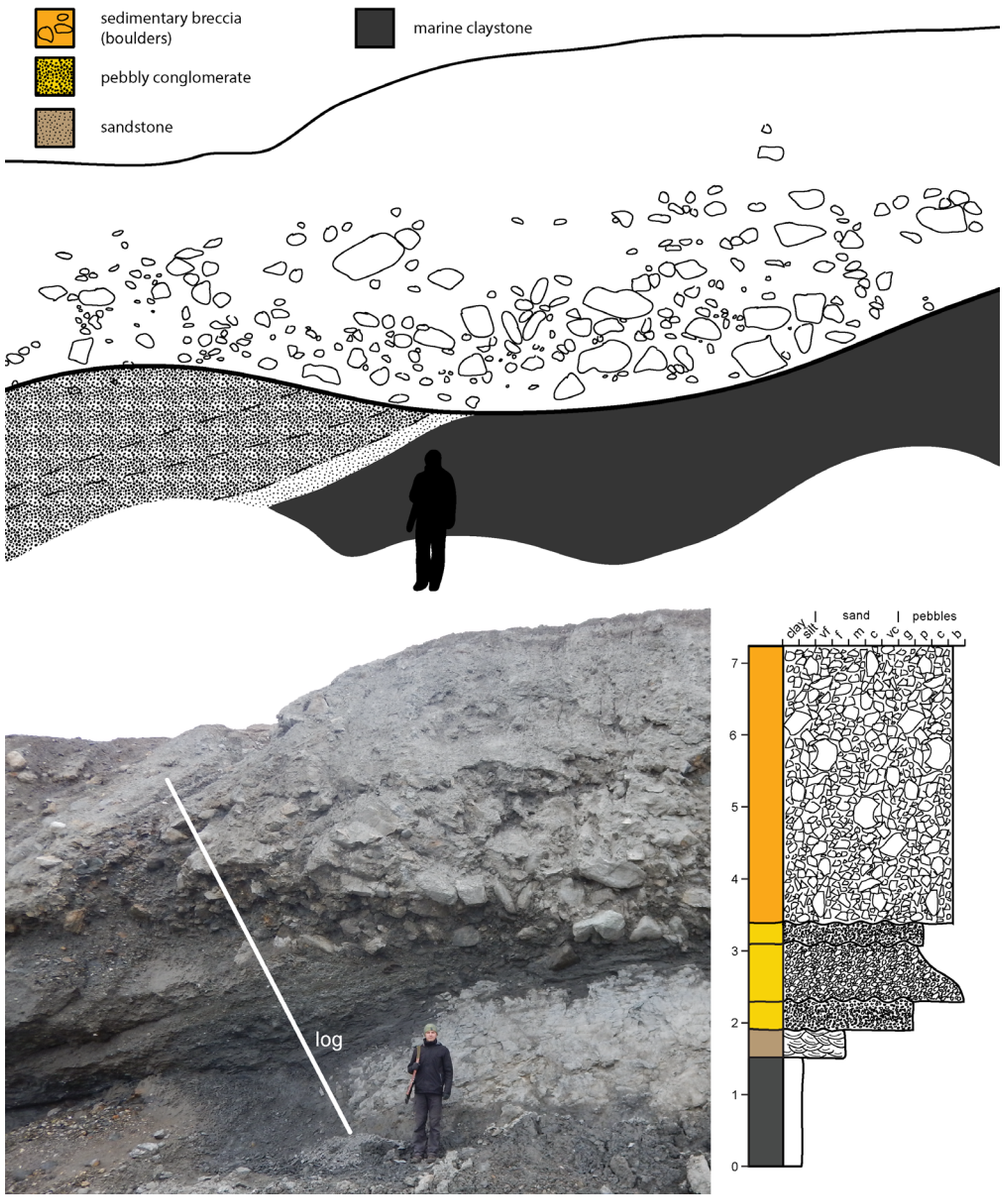

Figure 11. Photograph, line drawing and log of the type section of the Sarstangen conglomerate at Balanuspynten. Note the angular unconformity between the underlying finer-grained succession and the sedimentary breccia. Location: N 78.7214°, E 11.6816°.

Lithofacies association A eroded into a marine claystone through gravity flows, resulting in the occurrence of foraminifera and mud clasts (Fig. 8F). The clasts were probably not transported far as they are angular (Fig. 8F) and their source lithology is in direct contact with lithofacies association A (Fig. 11). However, the erosional contact with the underlying strata could also represent a major unconformity (Fig. 11), which would prohibit a direct correlation of the deposits. Therefore, we cannot be certain whether the lithofacies association was deposited under subaerial or submarine conditions. Based on the available data, we interpret the lithofacies association as the (subaerial) part of a debris-flow dominated fan delta.

Lithofacies association B: Fluvial (delta)

Description - Lithofacies association B comprises massive gravels and trough cross-bedded sandstones (Table 5). The layer boundaries within the lithofacies association are erosive (Fig. 11).

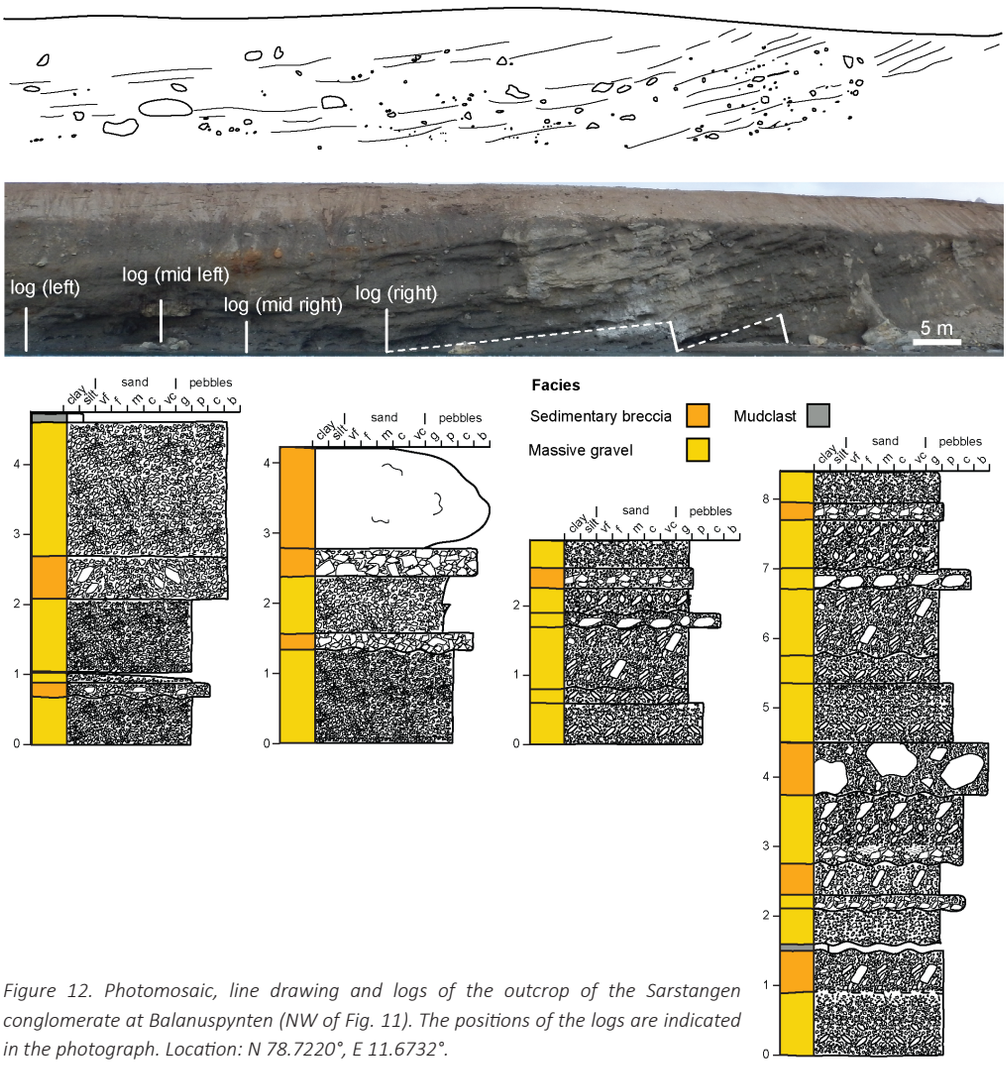

Figure 12. Photomosaic, line drawing and logs of the outcrop of the Sarstangen conglomerate at Balanuspynten (NW of Fig. 11). The positions of the logs are indicated in the photograph. Location: N 78.7220°, E 11.6732°.

Interpretation - Trough cross-bedding in the sandstone is a clear indicator of unidirectional flow in a deeper channel (Miall, 1977b; Walker & Cant, 1984) while coal fragments (Fig. 8G) indicate deposition in a terrestrial setting or tidal marsh (cf., Bloom, 1964). We, therefore, place the lithofacies association in a fluvial to deltaic environment. Deposition within a fluvio-deltaic system fits with the well-rounded, clast-supported texture of the conglomeratic units. Due to the contrast in depositional energy between the overlying breccia and the underlying marine claystone (Fig. 11), we favour a fan-delta environment.

Lithofacies association C: Marine offshore deposits

Description - Lithofacies association C comprises a marine claystone that contains well-rounded pebbles (Table 5; Fig. 8H).

Interpretation - We interpret lithofacies association C to represent a marine offshore deposit on the basis of marine foraminifera and its very fine-grained nature.

The pebbles are interpreted as dropstones. Dropstones are traditionally associated with transport by ice rafts (Spielhagen & Tripati, 2009) but can also be moved by wooden logs and kelp (Vogt & Parrish, 2012) or turbidity currents (Postma et al., 1988). The marine claystone was dated to a Lower-Middle Oligocene age (see below). At this time, the global climate transitioned from greenhouse (Eocene) to icehouse (Miocene) and Moran et al. (2006) reported ice-rafted dropstones in the high Arctic, i.e., the Lomonosov

Ridge, from as early as 45 Ma (Mid Eocene). Our analyses show that the paleoflora on the shores of the FG was indicative of a colder climate, consisting of Cupressaceae, Pinaceae and ferns (see below). Therefore, we cannot rule out that the pebbles were transported as ice-rafted debris.

Palynology

Despite the generally high organic content, only one (OSL–17–21; location: N 78.7214°, E 11.6816°) of the ten analysed samples contained palynomorphs that were sufficiently well preserved for analysis. The sample was obtained from the marine claystone in the Sarstangen conglomerate at Balanuspynten (Fig. 11). In these fine-grained sediments, we recognised a rich palynoflora and some diatoms. However, due to taphronomic processes the preservation is mostly poor, preventing an exact determination of palynomorphs at species level.

The assemblage is dominated by pollen of gymnosperms which are present in high diversity. The Pinaceae occur with pollen of *Pinus or Cathaya (Pityosporites labdacus).* Frequent is also the pollen of *Tsuga*, which is described from Spitsbergen as *Tsugaepollenites viridifluminipites* (Manum, 1962). Cupressaceae are also represented with different species of *Taxodium/Glyptostrobus (Inaperturopollenites* sp.) and *Sequoia (Sequoiapollenites* sp.). Compared to gymnosperm pollen, the fern spores and pollen grains of angiosperms are rare in the sample. Among the spores *Leiotriletes* sp. *(Schizaeaceae)* occurs regularly.

In the Arctic region, forests of the older Paleogene (Paleocene/Eocene) and forests of the younger Paleogene to Neogene (Oligocene/Miocene) can be distinguished. The latter are composed of conifers related to *Pinus, Picea, Tsuga* and *Taxodium*, with a minor element of angiosperms but relatively common ferns (Boulter & Manum, 1996). This composition is different from the Paleocene/Eocene floras that were also rich in conifers, but had a richer and more diverse angiosperm element and especially lacked *Tsuga* relatives (Boulter & Manum, 1996). Despite the generally poor preservation, we can confidently classify the sample as Lower to Middle Oligocene due to the occurrence of *Tsuga* and abundant other conifer pollen (Electronic Supplement 7).

For the Sarsbukta conglomerate, one coal sample (OSL–17–16; location: N 78.7263°, E 11.8430°) contains poorly preserved pollen, which prevent a stratigraphic classification. However, we found diatom fragments in the sample, which can probably be identified as remains of *Coscinodiscus.* This species occurs with a number of different species in records of the Upper Paleocene and Eocene in the North Sea basin (Mitlehner, 1996; Oreshkina, 2012) and may indicate a similar age for the Sarsbukta conglomerate. However, due to the degree of fragmentation and their occurrence in a terrestrial coal deposit it appears likely that the diatoms were reworked. In this case, the Sarsbukta conglomerate would be younger than Upper Paleocene/Eocene. For more information and photomicrographs of the palynomorphs see Electronic Supplement 7.

Structures in the Paleogene strata of the eastern Forlandsundet Graben

The data obtained from structures in the Paleogene strata include fault kinematics and regional-scale folding, as well as measurements of fracture planes in conglomerate clasts.

Faulting

A total of 176 fault planes were measured in the Sarsbukta conglomerate, and kinematics could be constrained for 70 of these (Fig. 4). The data show consistent NW–SE (~316° N) oriented tension axes throughout the study area (Fig. 4D, F). The style of faulting differs between the northern beach and central Sarsøyra. In central Sarsøyra, SE-dipping normal faults dominate. In addition to that, a WNW–ESE-oriented set of normal faults dipping NNE with a highly oblique dextral component is evident in the data from the northern beach (Fig. 4F).

The faults were likely active in a transtensional setting with the NW–SE main extension direction (~136° N) oriented at an angle of 20° towards the NNW–SSE (~336° N) trending basin-bounding lineaments (Fig. 1C). This interpretation is strongly supported by the oblique, normal-dextral displacements recorded by us from exposed parts of the main bounding faults in central Sarsøyra (Fig. 4B).

Folding

Based on a total of 50 bedding measurements we constructed the orientation of four, km–scale, open folds within the Sarsbukta conglomerate. The fold axes fall onto a NW–SE trend almost identical to the maximum elongation trend documented by the faults (Fig. 4). We interpret the folds to have formed in a transtensional setting since in transtension, folds rotate into parallellism with the main extension direction (e.g., Osmundsen & Andersen, 2001; Venkat-Ramani & Tikoff, 2002; Fossen et al., 2013).

We also observed a steepening of the strata towards the boundary fault at the northern beach which we interpret as drag folding or monoclinal bending.

Fractured clasts

In a distinct location at the northern beach (Fig. 4), clasts of all sizes are sliced by parallel mode-I fractures and injected with a coarse sandy matrix. The joints dip steeply and we determined a mean strike of 264° from 57 measurements (Fig. 13).

Tensional fracturing of clasts in a compliant matrix is not uncommon and often occurs in proximity to faults (Eidelman & Reches, 1992; Little, 1995; Little & Jones, 1998). The high contrast in Poisson ratio between a rigid clast and an unconsolidated matrix facilitates high tensional strain even in compressional settings. Only a few hundred metres of overburden are required to reach sufficient fracture pressures (Eidelman & Reches, 1992). Therefore, fracturing can occur shortly after deposition and before the sediment is lithified. Fracturing of the clasts appears parallel to the direction of main extension and has been used to determine paleostresses (Eidelman & Reches, 1992). However, Ramsay (1964) reported that clast fracture data are influenced by the geometry of adjacent faults.

Since fractured clasts are confined to a specific area on Sarsøyra, we regard them as a local feature. The mean orientation of fracture planes is 174° (Fig. 13) and is close to the 160° documented by Kleinspehn & Teyssier (2016).

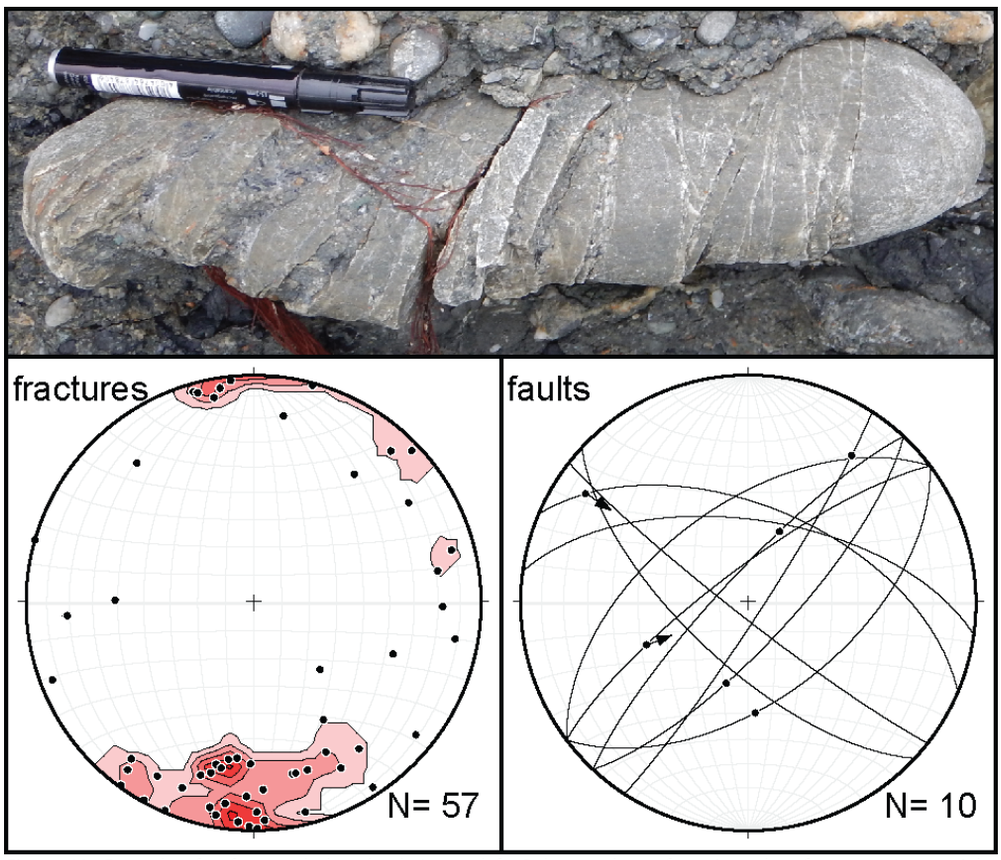

Figure 13. Example of a fractured clast (top). Lower left: Poles to planes from intraclast fractures. Lower right: Fault planes (lines), striations (poles) and kinematics (arrows) of faults in proximity to the fractured clasts. Location: N 78.7955° E 11.6874°.

Syntectonic features

Fig. 10B shows sedimentary layers of the Sarsbukta conglomerate in central Sarsøyra that steepen from the basin-bounding fault into the basin. These are overlain by wedge-shaped sedimentary bodies thickening away from the fault (Fig. 10A). The configuration differs from typical growth fault deposits that wedge towards the fault. We interpret that the sedimentary strata of the Sarsbukta conglomerate in central Sarsøyra formed an extensional monocline across the basin-bounding fault (Fig. 10B) (e.g., Gawthorpe & Leeder, 2000; Brandes & Tanner, 2014). The sedimentary wedges thickening towards the basin (Fig. 10A) represent the progradation of the depositional system on top of the monocline.

Along the northern beach, fine-grained floodplain sediments interfinger with coarse alluvial fan deposits (Figs. 4 & 9). We interpret the interfingering of sedimentary units to be caused by lateral migration of depositional elements due to cyclic movement along the bounding faults (e.g., Gawthorpe & Leeder, 2000; Ford et al., 2013).

Within the Sarstangen conglomerate, we interpret an angular unconformity (Fig. 11) as a synsedimentary feature. The underlying beds exhibit a dip of 20° towards the northwest while the fan deposits above dip between 12° and 17° to the west (Fig. 12). While the fan deposits may theoretically have maintained their depositional dip (Kleinspehn & Teyssier, 2016), the finer-grained lower beds were most likely deposited sub-horizontally. Consequently, the underlying succession was tilted prior to the deposition of the sedimentary breccia. Such folding could have been introduced by displacement gradients or drag along the proposed intrabasinal normal fault.

Discussion

Based on the available literature, we can establish a sequence of geological events as corner stones for the temporal evolution of the FG:

1. Onset of reverse and strike-slip faulting along the west coast of Spitsbergen between 55 Ma and 53 Ma, resulting in the formation of the WSFB (Bergh et al.,1997; Braathen et al., 1997; CASE Team, 2001; Engen et al., 2008; Faleide et al., 2008, 2015; Piepjohn et al., 2016).

2. Deposition of sedimentary units in the FG from ?44 Ma (Mid Eocene) to ?28 Ma (Mid Oligocene) and shift of the tectonic regime to transtension (Manum, 1960, 1962; Livsic, 1974, 1992; Lehmann et al., 1978; Feyling-Hanssen & Ulleberg, 1984; Steel et al., 1985; Manum & Throndsen, 1986; Čepek, 2001; Čepek & Krutzsch, 2001; Kleinspehn & Teyssier, 2016).

3. Onset of seafloor spreading at the Molloy Ridge segment at 22 Ma marking the end of rifting along the west coast of Spitsbergen (Engen et al., 2008).

The geochronological and structural data reported here, as well as some of the data presented in previous studies indicate that at least parts of the FG record transtensional crustal thinning which terminated with the formation of the Molloy Ridge west of PKF.

Deformation sequence on Sarsøyra

Our results support that three separate deformation phases affected the area of the eastern FG during the Paleogene:

From transpression to transtension (Eocene)

The transpressional stage of the WSFB (e.g., Braathen et al., 1997) is evident in fault measurements from basement rocks adjacent to the basin (Figs. 5 & 6C). The kinematics clearly show that deformation was dominated by ENE–WSW compression on NNW–SSE-oriented thrusts and strike-slip motion on NE–SW-oriented faults. In direct proximity to the eastern FG boundary, we document illite growth in a fault gouge at 53.5 ± 1.0 Ma. Provided the regional constraints, in particular the onset of North Atlantic seafloor spreading and dextral movements along the WSM at this time (Faleide et al., 2008), we find it likely that the K–Ar age dates a faulting event. The kinematics of the Engelskbukta Fault Zone which hosts the dated gouge indicate top-to-the-west reverse faulting, corresponding to backthrusting in the WSFB. Towards the Paleogene basin the fault rocks are overprinted by transtensional down-to-the-west movements. The Engelskbukta Fault Zone is probably a northern continuation of the Svartfjella-Eidembukta-Daudmannsodden lineament farther south (Maher et al. 1997), and thus represents a structure of regional importance.

The local occurrence of fractured clasts was used by Kleinspehn & Teyssier (2016) to argue for contractional or transpressional deformation of the Sarsbukta conglomerate within the WSFB. This would indicate that the oldest deposits in the study area formed prior to the onset of transtension. The well-rounded clasts in the sediments juxtaposed with the boundary fault and the apparent lack of angular blocks close to the fault scarp do not provide independent evidence regarding whether the Svartfjella-Eidembukta-Daudmannsodden fault system constituted the syn-depositional basin boundary.

Currently we cannot pinpoint when the regional stress field shifted from dextral transpression to dextral transtension. Our data show that this change introduced a transtensional tectonic regime under NW–SE-oriented extension to the WSM and the Forlandsundet area. Most of the structures in our study area reflect this style of deformation. In the basin fill exposed along the eastern FG boundary, outcrop-scale contractional structures are largely absent. Folds with similar axes orientation (NW–SE) as in Sarsøyra (Fig. 4) occur in the WSFB (e.g., Bergh et al., 1997, 2000) and the Central Basin (Paech, 2001) but are not representative as most of the WSFB structures strike NNW–SSE. The map-scale, open and gentle folds that we observe in our study area exhibit characteristic features of transtensional deformation. The fold axes are trending subparallel to the main extension direction (NW–SE) and a set of normal faults is oriented orthogonally to them (NE–SW; Fig. 4), recording hinge-parallel stretching. Therefore, we interpret them as transtensional folds (Fossen et al. 2013, see also Kleinspehn & Teyssier, 2016). This may indicate that most of the sediments along the eastern margin of the FG were deposited after the shift to a transtensional tectonic setting.

Sedimentation in the Sarsbukta conglomerate was dominated by two depositional systems which are evident from our sedimentological observations and the distribution of paleocurrent data (Fig. 4; von Gosen & Paech, 2001). These were gravelly alluvial fans and a sandy river system, respectively.

The interfingering architecture of conglomeratic units with finer-grained sediments along the northern beach (Figs. 4 & 9) could be attributed to variations in the availability of coarse sediment. In such a scenario, sediment supply may have been controlled by cyclic movement of the boundary fault and the resulting topographic relief in the footwall source area to the east (cf., Gawthorpe & Leeder, 2000). Alluvial fans sourced sediment transversely from the high-standing footwall in the east (Fig. 14). In the basin itself, there was an axial river with a gravelly bedload and an associated floodplain (Fig. 14). Sediment thickness variations adjacent to the bounding fault can be interpreted in terms of a syn-depositional, extensionally forced monocline (Fig. 10A, B) and may also point towards syn-sedimentary transtension. Steepening of the interfingering strata towards the basin boundary (Fig. 4) was probably caused by monoclinal bending or normal fault drag. In summary, our sedimentological data allow for a deposition of the Sarsbukta conglomerate before, after or during the shift to transtension.

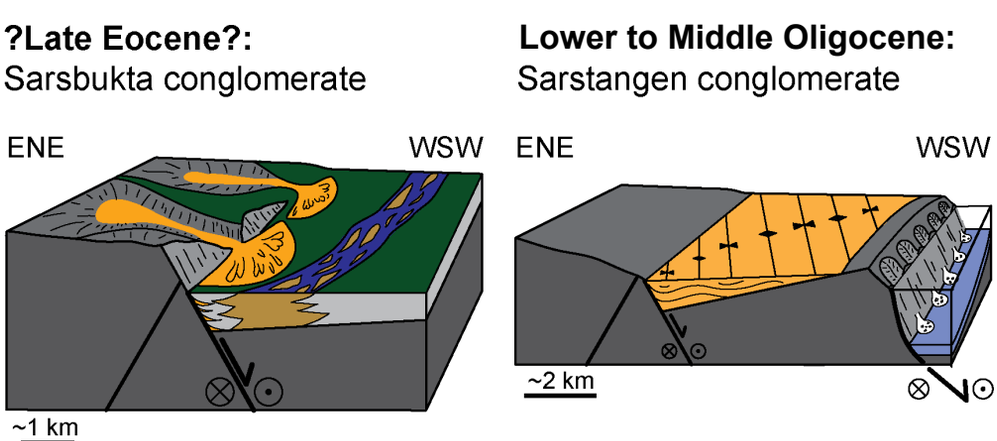

Figure 14. Schematic models for the tectono-sedimentary evolution of Sarsøyra under progressive dextral transtension. The Sarsbukta conglomerate consists of footwall-derived alluvial fans interacting with an axial fluvial system. It was subsequently folded during the deposition of the Sarstangen conglomerate. The Sarstangen conglomerate consists of marine fines and fan deposits off a high-standing fault scarp. Note that the orientation is ENE–WSW, i.e., looking towards the south.

Progressive transtensional rifting (Oligocene)

Subsequent to its deposition, the Sarsbukta conglomerate was deformed in a transtensional setting as manifested in our fault kinematic data and by transtensional folding throughout the study area (Fig. 4).

The Sarstangen conglomerate is interpreted to have evolved under the same transtensional stress field as the one that deformed the Sarsbukta conglomerate, i.e., NW–SE-oriented extension. The Sarstangen conglomerate is interpreted to have been deposited along an intrabasinal normal fault that exhibits a throw of >1 km (Kleinspehn & Teyssier, 2016; Electronic Supplement 6). However, it does not appear to have been affected by the internal deformation recorded by the Sarsbukta conglomerate. The angular unconformity within the Sarstangen conglomerate (Fig. 11) may indicate that sedimentation was contemporaneous with differential displacement along the fault. Sudden fault movement created high relief and the associated seismicity that gave rise to rock falls.

The formation of the WSM terminated at around 22 Ma when the first oceanic crust formed between Greenland and Svalbard (Engen et al., 2008). Until then, progressive thinning of the lithosphere occurred as fault activity migrated towards the west, away from the Forlandsundet area.

Evolution of the Forlandsundet Graben

In the following, we discuss the implications of our findings with respect to the evolution of the entire FG and the WSM.

Our fission track results (KKF–11 & KKF–18; Fig. 7) generally support a differential thermal history across the FG that is also inferred from the available vitrinite reflectance data (Fig. 3 A, B; e.g., Paech & Koch, 2001). The Paleogene deposits on the PKF experienced much higher temperatures compared to their eastern counterparts. A deeper burial and subsequent exhumation of the strata on PKF could explain this gradient in maturity. Kleinspehn & Teyssier (1992) speculated that parts of the metamorphic rocks on PKF were exhumed as a metamorphic core complex during crustal thinning. This concept would be in line with the thermal modelling results of Barnes & Schneider (2018; Fig. 7) who suggested a late and fast exhumation of the PKF. However, Kleinspehn & Teyssier (1992) pointed towards the apparent lack of a major detachment in the Caledonian basement on PKF. As stated previously (see Geological background), the Bouréefjellet Fault Zone could theoretically represent such a low-angle detachment, related to an underlying metamorphic core complex (sensu Hossack, 1984; Braathen et al., 2018). To test this hypothesis, extensive field- and thermochronological work on the relationship of the so-called Pinkiefjellet Unit to surrounding rocks would be required. Existing literature have, however, attributed reverse kinematics to the Bouréefjellet Fault Zone (Hjelle et al., 1999; Schneider et al., 2018), so an interpretation as a metamorphic core complex is not evident from published work.

The relationship of the Paleogene deposits on PKF to the sedimentary rocks in our study area remains uncertain. In addition to having experienced significantly higher temperatures, they exhibit a higher degree of structural complexity, characterised by tight, overturned folding and thrust faulting (Gabrielsen et al., 1992; von Gosen & Paech, 2001). With this in mind, we can establish two end-member models for the formation of the FG as a whole.

The striking differences in structural and thermal appearance between the eastern and western basin margins could be explained with a two-stage evolution of the FG. In such a scenario, the shift from transpression to transtension would likely have occurred between the times of deposition of the sedimentary units along the western and eastern basin margins. Hence, the sedimentary rocks on

the PKF would have been deposited in a piggyback basin within the WSFB, tentatively experiencing compressional deformation and subsequent burial. If this occurred prior to, or during deposition of the Sarsbukta conglomerate along the eastern basin margin, the differential thermal imprint could be explained by differential burial followed by transtensional exhumation. Whether the sedimentary rocks on PKF could potentially be correlated to the exposed Paleogene strata at Sarsøyra depends on when the Sarsbukta conglomerate was deposited. If it was deposited in a piggyback basin, rocks of that age may be present on PKF. If the sedimentation of the Sarsbukta conglomerate, however, happened in a transtensional setting, the sedimentary rocks on PKF cannot be correlated as the exposed Paleogene units on Sarsøyra would be younger in their entirety.

An interesting alternative to the two-stage evolution of the FG is that the compressional structures along the western basin margin developed as a result of partitioned transtension (sensu De Paola et al., 2005). Strain partitioning offers an elegant explanation for structural complexity in sedimentary basins. Adjacent to the SFZ, e.g., in the Sørvestsnaget Basin, partitioning of transtensional strain into compressional and extensional structures has been documented by Kristensen et al. (2017). To be able to compare the basin evolution in the FG (WSM) with that of the Sørvestsnaget Basin (SFZ; Mjelde et al., 2002; Kristensen et al., 2017), we have to consider the basins in their larger-scale spatial and temporal context. Despite their first-order similar tectonic setting along the transform margin of the Barents Sea, the timing of margin formation was different in the two basin locations. The SFZ was active from the breakup in the Norwegian Sea from Early Eocene, with southern parts of the Sørvestsnaget Basin reaching rift climax in the Late Paleocene to Lower Eocene and the northern part in Mid Eocene (Kristensen et al., 2017). At that time, the Eurekan orogeny affected the WSM and margin formation commenced from Early Eocene time (Faleide et al., 2008) with rifting in the FG climaxing in Early to Mid Oligocene during the deposition of the Sarstangen conglomerate. Despite the fact that the SFZ did not experience a mountain building event like the WSM, Kristensen et al. (2017) recognise major thrust faults and folding in the Sørvestsnaget Basin. They concluded that the thrusts along with folds and normal faults evolved under highly oblique transform movements (angle of divergence between α=7.78° and α=10.54°; Kristensen et al., 2017). Our kinematic assessment suggests an angle of divergence around 20° for the FG (orientation FG 336° N, T-axis 316° N) which resembles the divergence angle we derived from published plate-motion flowlines (Engen et al., 2008). This means that the tectonic setting of the FG was right on the threshold between wrench- (α<20°) and extension- (α>20°) dominated transtension. The horizontal shortening associated with wrench dominated transtension is considered to be sufficient to introduce compressive structures, including thrusts, conjugate strike-slip faults and folds (De Paola et al., 2005, and references therein). On the basis of cross-cutting relationships, von Gosen & Paech (2001) suggested that normal faults were reactivated under compression on PKF. As there is no indication for a compressional episode after the extensional, these structures may hint towards coeval extension and shortening under transtension. Thus, there is a possibility that a part of or the entire Paleogene succession in the FG was deposited and deformed under strain-partitioned progressive transtension. In that case, the Paleogene stratigraphy along both shores of Forlandsundet could be of the same age and potentially be correlated. However, it is probable that the units with higher structural complexity represent older rocks because they had more time to accumulate strain. As proposed for the two-stage model, differential burial and exhumation could have caused the maturity gradients observed across the FG. In addition, convective heat flow along the western basin margin, possibly induced by the propagation of the mid-oceanic ridge (Paech & Koch, 2001), may have contributed.

Further implications

The FG developed in a tectonic framework along the WSM comparable to that of other basins along the NE Atlantic transform margin. It could therefore provide a valuable onshore analogue for these

offshore basins as well as for basins along other transform margins. Comparing the FG to the Sørvestsnaget Basin adjacent to the SFZ (Mjelde et al., 2002; Kristensen et al., 2017), we recognise similarities in the deformation style. In particular, both basins exhibit transtensional folds with axes oriented parallel to the main extension direction. Kristensen et al. (2017) further document seismic-scale normal faulting perpendicular to the fold axes. We observe a similar relationship between outcrop-scale normal faults and folds in the Paleogene strata on Sarsøyra (Fig. 4). Normal faulting on scales as in the Sørvestsnaget Basin, however, is not apparent within the sedimentary infill of the FG. Thrust faulting and tight folding are present in the sedimentary succession along the western basin boundary of the FG (Lepvrier, 1990; Gabrielsen et al., 1992; von Gosen & Paech, 2001). Even though cross-cutting relationships might indicate transtensional deformation, the variance in the published orientation data is high. Therefore, we cannot currently attribute compressive structures on PFK solely to strain-partitioned transtension as Kristensen et al. (2017) did for the Sørvestsnaget Basin.

In more general terms, the FG and the Sørvestsnaget Basin share an analogous deformation history characterised by complex syn- to post-depositional deformation. In the FG, this is demonstrated by the Sarsbukta conglomerate, which may have been deposited along the basin-bounding oblique normal fault and subsequently folded under progressive transtension. Equally complicated deformation patterns have been documented in transtensional basins elsewhere, e.g., the Santa Rosa basin in Baja California (Seiler et al., 2010) or the Devonian basins of western Norway (Osmundsen & Andersen, 2001). We therefore propose that complex transtensional deformation histories as those exemplified by the FG and the Sørvestsnaget Basin may be common along obliquely rifted margins and other large-scale transform boundaries.

Conclusions

Based on our results and discussion we conclude that:

• Basins that evolve along obliquely rifted margins can be characterised by complex syn- to post-depositional deformation.

• The deformation sequence on Sarsøyra throughout the Paleogene includes reverse faulting at 53.5 ± 1.0 Ma likely connected to the formation of the WSFB. The Sarsbukta conglomerate was deposited in a piggyback basin within the WSFB or after the shift to NW–SE transtension. It was then deformed under progressive transtension while the Sarstangen conglomerate was being deposited in Early–Mid Oligocene time. Rifting in the continental domain ceased with the establishment of the passive margin at 22 Ma.

• The older Sarsbukta conglomerate consists of marginal alluvial-fan sediments, interfingering with fluvial and floodplain deposits. It experienced transtensional deformation, i.e., folding and normal faulting, with a NW–SE-oriented oblique extension trend.

• The younger Sarstangen conglomerate consists of a marine claystone, overlain by a proximal fan deposit most likely derived from an uplifted footwall. Its fossil content suggests an Early–Mid Oligocene age.

Acknowledgements. We especially thank our field assistants Julian Janocha, Kristine Larssen, Tim Hake and Erik Kuschel for their support, even during long, wet and cold days with polar bears around. This study was funded by the Norwegian Research Council through Arctic Field Grants from the Svalbard Science Forum, the University of Oslo, the Research Centre for Arctic Petroleum Exploration (ARCEx), the Geological Survey of Norway and the University Centre in Svalbard. The Czech Arctic Research Station of the University of South Bohemia and the Logistics Department of the University Centre in Svalbard provided logistical support as well as equipment. We thank Thomas B. Kristensen and Owen Anfinson for their constructive reviews that improved the quality of the manuscript.

References

Allmendinger, R.W., Cardozo, N.C. & Fisher, D. 2013: *Structural Geology Algorithms: Vectors and Tensors.* Cambridge University Press, Cambridge, England.

Andresen, A., Haremo, P., Swensson, E. & Bergh, S.G. 1992: Structural geology around the southern termination of the Lomfjorden Fault Complex, Agardhdalen, east Spitsbergen. *Norwegian Journal of Geology 72,* pp. 83–91.

Barker, C.E. & Pawlewicz, M.J. 1994: Calculation of Vitrinite Reflectance from Thermal Histiries amd Peak Temperatures. A comparison of Methods. Vitrinite reflectance as a maturity parameter: aplications and limitations. *ACS Symposium Series 570,* pp. 216–229. https://doi.org/10.1021/bk-1994-0570.ch014

Barnes, C. & Schneider, D. 2018: Late Cretaceous − Paleogene burial and exhumation history of the Southwestern Basement Province, Svalbard, revealed by zircon (U–Th)/ He thermochronology, *In:* Piepjohn, K., Strauss, J. V, Reinhardt, L. & McClelland, W.C. (eds.): *Circum-Arctic Structural Events: Tectonic Evolution of the Arctic Margins and Trans-Arctic Links with Adjacent Orogens,* Geological Society of America Special Paper, Geological Society of America, pp. 1–22. https://doi.org/10.1130/2018.2541(07)

Bergh, S.G., Braathen, A. & Andresen, A. 1997: Interaction of basement-involved and thin-skinned tectonism in the Tertiary fold-thrust belt of central Spitsbergen, Svalbard. *AAPG Bulletin 81,* pp. 637–661.

Bergh, S.G., Braathen, A., Karlson, F. & Maher, H.D. 1999: *Fault Motion Along the Eastern Margin of the Forlandsundet graben, Sarstangen, Svalbard.* Preliminary report, University of Nebraska at Omaha, 10 pp.

Bergh, S.G., Maher, H.D. & Braathen, A. 2000: Tertiary divergent thrust directions from partitioned transpression, Broggerhalvoya, Spitsbergen. *Norwegian Journal of Geology 80,* pp. 63–81. https://doi.org/10.1080/002919600750042573

Bernet, M. 2005: Fission-track Analysis of Detrital Zircon. *Reviews in Mineralogy and Geochemistry 58*, pp. 205–237. https://doi.org/10.2138/rmg.2005.58.8

Betlem, P., Midttømme, K., Jochmann, M., Senger, K. & Olaussen, S. 2018: Geothermal Gradients on Svalbard, Arctic Norway. *First EAGE/IGA/DGMK Joint Workshop on Deep Geothermal Energy 2018, 8–9 November.* pp. 9–11. https://doi.org/10.3997/2214-4609.201802945

Blair, T.C. & McPherson, J.G. 1994: Alluvial Fans and their Natural Distinction from Rivers Based on Morphology, Hydraulic Processes, Sedimentary Processes, and Facies Assemblages. J*ournal of Sedimentary Research 64A,* pp. 450–489.
https://doi.org/10.1306/D4267DDE-2B26-11D7-8648000102C1865D

Blinova, M., Thorsen, R., Mjelde, R. & Faleide, J.I. 2009: Structure and evolution of the Bellsund graben between Forlandsundet and Bellsund (Spitsbergen) based on marine seismic data. *Norwegian Journal of Geology 89,* pp. 215–228.

Bloom, L.A. 1964: Peat Accumulation and Compaction in a Connecticut Coastal Marsh. *Journal of Sedimentary Research 34,* pp. 599–603.
https://doi.org/10.1306/74D710F5-2B21-11D7-8648000102C1865D

Blythe, A.E., & Kleinspehn, K.L. 1998: Tectonically versus climatically driven Cenozoic exhumation of the Eurasian plate margin, Svalbard: Fission track analyses. *Tectonics 17,* pp. 621–639.
https://doi.org/10.1029/98TC01890

Boulter, M.C. & Manum, S.B. 1996: OLIGOCENE AND MIOCENE VEGETATION IN HIGH LATITUDES OF THE NORTH ATLANTIC: PALYNOLOGICAL EVIDENCE FROM THE HOVGÅRD RIDGE IN THE GREENLAND SEA (SITE 908). *Proceedings of the Ocean Drilling Program, Scientific Results 151,* pp. 289–296.
https://doi.org/10.2973/odp.proc.sr.151.111.1996

Braathen, A. & Bergh, S.G. 1999: Application of a critical wedge taper model to the Tertiary transpressional fold-thrust belt on Spitsbergen, Svalbard. *GSA Bulletin 111*, pp. 2–19.

Braathen, A., Bergh, S.G. & Maher, H.D. 1997: Thrust kinematics in the central part of the Tertiary transpressional fold-thrust belt in Spitsbergen. *NGU Bulletin 433*, pp. 32–33.

Braathen, A., Osmundsen, P.T., Maher, H.D. & Ganerød, M. 2018: The Keisarhjelmen detachment records Silurian–Devonian extensional collapse in Northern Svalbard. *Terra Nova 30,* pp. 34–39.
https://doi.org/10.1111/ter.12305

Brandes, C. & Tanner, D.C. 2014: Fault-related folding: A review of kinematic models and their application. *Earth-Science Reviews 138,* pp. 352–370. https://doi.org/10.1016/j.earscirev.2014.06.008

Brune, S., Williams, S.E. & Müller, D.R. 2018: Oblique rifting: the rule, not the exception. *Solid Earth Discussions 9,* pp. 1187–1206. https://doi.org/10.5194/se-9-1187-2018

Campion, K.M., Sprague, A.R., Mohrig, D.C., Lovell, R.W., Drzewiecki, P.A., Sullivan, M.D., Ardill, J.A., Jensen, G.N. & Sickafoose, D.K. 2000: Outcrop Expression of Confined Channel Complexes. *In:* Weimer, P. (ed.), *Deep-Water Reservoirs of the World,* SEPM Society for Sedimentary Geology, pp. 13–36.
https://doi.org/10.5724/gcs.00.15.0127

CASE Team 2001: The Evolution of the West Spitsbergen Fold-and-Thrust Belt. *In:* Tessensohn, F. (ed.): *Intra-Continental Fold Belts: CASE 1, Spitsbergen,* Schweizerbart Science Publishers, pp. 733–773.

Čepek, P. 2001: Paleogene calcareous nannofossils from the Firkanten and Sarsbukta Formations on Spitsbergen. *In:* Tessensohn, F. (ed.): *Intra-Continental Fold Belts: CASE 1, Spitsbergen,* Schweizerbart Science Publishers, pp. 535–547.

Čepek, P. & Krutzsch, W. 2001: Conflicting interpretations of the Tertiary biostratigraphy of Spitsbergen and new palynological results: *In:* Tessensohn, F. (ed.): *Intra-Continental Fold Belts: CASE 1, Spitsbergen,* Schweizerbart Science Publishers, pp. 551–599.

Dallmann, W.K., Dypvik, H., Gjelberg, J.G., Harland, W.B., Johannessen, E.P., Keilen, H.B., Larssen, G.B., Lønøy, A., Midbøe, P.S., Mørk, A., Nagy, J., Nilsson, I., Nøttvedt, A., Olaussen, S., Pcelina, T.M., Steel, R.J. & Worsley, D. 1999: *Lithostratigraphic lexicon of Svalbard: review and recommendations for nomenclature use: Upper Palaeozoic to Quaternary bedrock.* Norwegian Polar Institute, Tromsø.

Dallmann, W.K., Blomeier, D., Elvevold, S., Mørk, A., Olaussen, S., Grundvåg, S.-A., Bond, D. & Hormes, A. 2015: Historical geology. *In:* Dallmann, W.K. (ed.): *Geoscience Atlas of Svalbard,* Norwegian Polar Institute, Tromsø, pp. 89–131.

De Paola, N., Holdsworth, R.E., McCaffrey, K.J.W. & Barchi, M.R. 2005: Partitioned transtension: An alternative to basin inversion models. *Journal of Structural Geology 27*, pp. 607–625. https://doi.org/10.1016/j.jsg.2005.01.006

Díaz-Azpiroz, M., Brune, S., Leever, K.A., Fernández, C. & Czeck, D.M. 2016: Tectonics of oblique plate boundary systems. *Tectonophysics 693*, pp. 165–170. https://doi.org/10.1016/j.tecto.2016.07.028

Dörr, N., Lisker, F., Clift, P.D., Carter, A., Gee, D.G., Tebenkov, A.M. & Spiegel, C. 2012: Late Mesozoic-Cenozoic exhumation history of northern Svalbard and its regional significance: Constraints from apatite fission track analysis. *Tectonophysics 514*, pp. 81–92. https://doi.org/10.1016/j.tecto.2011.10.007

Døssing, A., Hopper, J.R., Olesen, A. V., Rasmussen, T.M. & Halpenny, J. 2013: New aero-gravity results from the Arctic: Linking the latest Cretaceous-early Cenozoic plate kinematics of the North Atlantic and Arctic Ocean. *Geochemistry, Geophysics, Geosystems 14,* pp. 4044–4065. https://doi.org/10.1002/ggge.20253

Eidelman, A. & Reches, Z. 1992: Fractured pebbles — A new stress indicator. *Geology 20,* pp. 307–310. https://doi.org/10.1130/0091-7613(1992)020%3C0307:FPANSI%3E2.3.CO;2

Engen, Ø., Faleide, J.I. & Dyreng, T.K. 2008: Opening of the Fram Strait gateway: A review of plate tectonic constraints. *Tectonophysics 450*, pp. 51–69. https://doi.org/10.1016/j.tecto.2008.01.002

Faleide, J.I., Tsikalas, F., Breivik, J., Mjelde, R., Ritzmann, O., Engen, O., Wilson, J. & Eldholm, O. 2008: Structure and evolution of the continental margin off Norway and the Barents Sea. *Episodes 31,* pp. 82–91. https://doi.org/10.18814/epiiugs/2008/v31i1/012

Faleide, J.I., Bjorlykke, K. & Gabrielsen, R.H. 2015: Geology of the Norwegian Continental Shelf. *In:* Bjorlykke, K. (ed.): *Petroleum Geoscience.* Springer-Verlag Berlin Heidelberg, pp. 603–637. https://doi.org/10.1007/978-3-642-34132-8_25

Feyling-Hanssen, R.W. & Ulleberg, K. 1984: A Tertiary-Quaternary section at Sarsbukta, Spitsbergen, Svalbard, and its foraminifera. *Polar Research 2,* pp. 77–106. https://doi.org/10.3402/polar.v2i1.6963

Ford, M., Rohais, S., Williams, E.A., Bourlange, S., Jousselin, D., Backert, N. & Malartre, F. 2013: Tectono-sedimentary evolution of the western Corinth rift (Central Greece). *Basin Research 25,* 3–25. https://doi.org/10.1111/j.1365-2117.2012.00550.x

Fossen, H., Teyssier, C. & Whitney, D.L. 2013: Transtensional folding. *Journal of Structural Geology 56,* pp. 89–102. https://doi.org/10.1016/j.jsg.2013.09.004

Gabrielsen, R.H., Kløvjan, O.S., Haugsbø, H., Midbøe, P.S., Nøttvedt, A., Rasmussen, E. & Skott, P.H. 1992: A structural outline of the Forlandsundet Graben, Prins Karls Forland, Svalbard. *Norwegian Journal of Geology 72,* pp. 105–120.

Gallagher, K., Brown, R. & Johnson, C. 1998: Fission Track Analysis and Its Applications To Geological Problems. *Annual Review of Earth and Planetary Sciences 26,* pp. 519–572. https://doi.org/10.1146/annurev.earth.26.1.519

Gawthorpe, R.L. & Leeder, M.R. 2000: Tectono-sedimentary evolution of active extensional basins. *Basin Research 12,* pp. 195–218. https://doi.org/10.1111/j.1365-2117.2000.00121.x

Goscombe, B.D. & Passchier, C.W. 2002: Asymmetric boudins as shear sense indicators - an assessment from field data. *Journal of Structural Geology 25,* pp. 1–15. https://doi.org/10.1016/S0191-8141(02)00045-7

Helland-Hansen, W. & Grundvåg, S.A. 2020: The Svalbard Eocene-Oligocene (?) Central Basin succession: Sedimentation patterns and controls. *Basin Research,* pp. 1–25. https://doi.org/10.1111/bre.12492

Henriksen, E., Ryseth, A.E., Larssen, G.B., Heide, T., Rønning, K., Sollid, K. & Stoupakova, A.V. 2011: Chapter 10 Tectonostratigraphy of the greater Barents Sea: implications for petroleum systems. *In:* Spencer, A.M., Embry, A.F., Gautier, D.L., Stoupakova, A.V. & Sørensen, K. (eds.): *Arctic Petroleum Geology.* The Geological Society, London, pp. 163-195. https://doi.org/10.1144/M35.10

Hjelle, A., Piepjohn, K., Saalmann, K., Ohta, Y., Salvigsen, O., Thiedig, F. & Dallmann, W.K. 1999: Geological Map Svalbard, A7G Kongsfjorden, scale 1:100,000, N*orwegian Polar Institute.*

Hossack, J.R. 1984: The geometry of listric growth faults in the Devonian basins of Sunnfjord, W Norway. *Journal of the Geological Society 141,* pp. 629–637. https://doi.org/10.1144/gsjgs.141.4.0629

Hosseinpour, M., Müller, D.R., Williams, S.E. & Whittaker, J.M. 2013: Full-fit reconstruction of the labrador sea and baffin bay. *Solid Earth 4,* pp. 461–479. https://doi.org/10.5194/se-4-461-2013

Jakobsson, M., Mayer, L., Coakley, B., Dowdeswell, J.A., Forbes, S., Fridman, B., Hodnesdal, H., Noormets, R., Pedersen, R., Rebesco, M., Schenke, H.W., Zarayskaya, Y., Accettella, D., Armstrong, A., Anderson, R.M., Bienhoff, P., Camerlenghi, A., Church, I., Edwards, M., Gardner, J. V, Hall, J.K., Hell, B., Hestvik, O., Kristoffersen, Y., Marcussen, C., Mohammad, R., Mosher, D., Nghiem, S. V, Pedrosa, M.T. & Travaglini, P.G. 2012: The International Bathymetric Chart of the Arctic Ocean (IBCAO) Version 3.039. https://doi.org/10.1029/2012GL052219

Jochmann, M.M., Augland, L.E., Lenz, O., Bieg, G., Haugen, T., Grundvåg, S.A., Jelby, M.E., Midtkandal, I., Dolezych, M. & Hjálmarsdóttir, H.R. 2019. Sylfjellet: a new outcrop of the Paleogene Van Mijenfjorden Group in Svalbard. *arktos,* pp. 1–22. https://doi.org/10.1007/s41063-019-00072-w

Kaiser, H. & Ashraf, A.R. 1974: Gewinnung und Präparation fossiler Sporen und Pollen sowie anderer Palynomorphae unter besonderer Betonung der Siebmethode. *Geologisches Jahrbuch 25,* pp. 85–114.

Kanat, L. & Morris, A. 1988: A working stratigraphy for central western Oscar II Land, Spitsbergen. *Norsk Polarinstitutt Skrifter 190,* pp. 5–23.

Kesper, J. 1986: *Kartierung der tertiären Ablagerungen auf Sarsöyra (Svalbard).* Unpublished diploma thesis, Universität Kiel, 63 pp.

Kleinspehn, K.L. & Teyssier, C. 1992: Tectonics of the Paleogene Forlandsundet Basin, Spitsbergen - a Preliminary-Report. *Norwegian Journal of Geology 72,* pp. 93–104.

Kleinspehn, K.L. & Teyssier, C. 2016: Oblique rifting and the Late Eocene–Oligocene demise of Laurasia with inception of Molloy Ridge: Deformation of Forlandsundet Basin, Svalbard. *Tectonophysics 693,* pp. 363–377. https://doi.org/10.1016/j.tecto.2016.05.010

Krasilscikov, A.A., Kubanskij, A.P. & Ohta, Y. 1995: Surface Magnetic Anomaly Study on the Eastern Part of the Forlandsundet-Graben. *Polar Research 14,* pp. 55–68.
https://doi.org/10.3402/polar.v14i1.6651

Kristensen, T.B., Rotevatn, A., Marvik, M., Henstra, G.A., Gawthorpe, R.L., & Ravnås, R., 2017: Structural evolution of sheared margin basins: The role of strain partitioning. Sørvestsnaget Basin, Norwegian Barents Sea. Basin Research 1–23. https://doi.org/10.1111/bre.12253

Kübler, B. 1967: La cristallinité de l'illite et les zones tout à fait supérieures du métamorphisme. *In:* Etages Tectoniques. Colloque de Neuchâtel, pp. 105–121.

Leeder, M.R. & Gawthorpe, R.L. 1987: Sedimentary models for extensional tilt-block/half-graben basins. *Geological Society, London, Special Publications 28,* pp. 139–152.
https://doi.org/10.1144/GSL.SP.1987.028.01.11

Leever, K.A., Gabrielsen, R.H., Faleide, J.I. & Braathen, A. 2011: A transpressional origin for the West Spitsbergen fold-and-thrust belt: Insight from analog modeling. *Tectonics 30*, pp. 1–24.
https://doi.org/10.1029/2010TC002753

Lehmann, U., Thiedig, F. & Harland, W.B. 1978: Spitzbergen im Tertiär. *Polarforschung 48,* pp. 120–138.

Lepvrier, C. 1990: Early Tertiary Paleostress History and Tectonic Development of the Forlandsundet Basin, Svalbard, Norway. *Norsk Polarinstitutt Meddelelser 112,* pp. 3–16.

Lister, G.S. & Davis, G.A. 1989: The origin of metamorphic core complexes and detachment faults formed during Tertiary continental margins. pp. 246–250.

Little, T.A. 1995: Brittle deformation adjacent to the Awatere strike-slip fault in New Zealand: Faulting patterns, scaling relationships, and displacement partitioning. *GSA Bulletin 107*, pp. 1255–1271.
https://doi.org/10.1029/2010TC002753

Little, T.A. & Jones, A. 1998: Seven million years of strike-slip and related off-fault deformation, northeastern Marlborough fault system, South Island, New Zealand. *Tectonics 17,* pp. 285–302.
https://doi.org/10.1029/97TC03148

Livsic, J. 1974: Palaeogene deposits and the platform structure of Svalbard. Norsk Polarinstitutt Skrifter 159, pp. 5–51.

Livsic, J. 1992: Tectonic history of Tertiary sedimentation of Svalbard. *Norwegian Journal of Geology 72,* pp. 121–127.

Maher, H.D., Bergh, S.G., Braathen, A. & Ohta, Y. 1997: Svartfjella, Eidembukta, and Daudmannsodden lineament: Tertiary orogen-parallel motion in the crystalline hinterland of Spitsbergen's fold-thrust belt. *Tectonics 16,* pp. 88–106. https://doi.org/10.1029/96TC02616

Manum, S.B. 1960: Some dinoflagellates and hystrichosphaerids from the Lower Tertiary of Spitsbergen. *Nytt Magasin for Botanikk 8,* pp. 17–21.

Manum, S.B. 1962: Studies in the Tertiary flora of Spitsbergen, with notes on Tertiary floras of Ellesmere Island, Greenland, and Iceland. *Norsk Polarinstitutt Skrifter 125,* pp. 1–127.

Manum, S.B. & Throndsen, T. 1986: Age of Tertiary formations on Spitsbergen. *Polar Research 4,* pp. 103–131. https://doi.org/10.1111/j.1751-8369.1986.tb00526.x

Marrett, R. & Allmendinger, R.W. 1990: Kinematic analysis of fault-slip data. *Journal of Structural Geology 12*, pp. 973–986. https://doi.org/10.1016/0191-8141(90)90093-E

McCann, A.J. & Dallmann, W.K. 1996: Reactivation history of the long-lived Billefjorden Fault Zone in north central Spitsbergen, Svalbard. *Geological Magazine 133*, pp. 63–84. https://doi.org/10.1017/S0016756800007251

Miall, A.D. 1977a: Lithofacies types and vertical profile models in braided river deposits: a summary. *Fluvial Sedimentology 5*, pp. 597–600.

Miall, A.D. 1977b: A Review of the Braided-River Depositional Environment. *Earth Science Reviews 13,* pp. 1–62. https://doi.org/10.1016/0012-8252(77)90055-1

Miall, A.D. 1985: Architectural-Element Analysis: A New Method of Facies Analysis Applied to Fluvial Deposits. *Earth-Science Reviews 22,* pp. 261–308. https://doi.org/10.1016/00128252(85)90001-7

Mitlehner, A.G. 1996: Palaeoenvironments in the North Sea Basin around the Paleocene–Eocene boundary: evidence from diatoms and other siliceous microfossils. *Geological Society, London, Special Publication 101,* pp. 255–273. https://doi.org/10.1144/GSL.SP.1996.101.01.15

Mjelde, R., Breivik, A.J., Elstad, H., Ryseth, A.E., Skilbrei, J.R., Opsal, J.G., Shimamura, H., Murai, Y. & Nishimura, Y. 2002: Geological development of the Sørvestsnaget Basin, SW Barents Sea, from ocean bottom seismic, surface seismic and potential field data. *Norwegian Journal of Geology 82*, pp. 183–202.

Moran, K., Backman, J., Brinkhuis, H., Clemens, S.C., Cronin, T., Dickens, G.R., Eynaud, F., Gattacceca, J., Jakobsson, M., Jordan, R.W., Kaminski, M., King, J., Koc, N., Krylov, A., Martinez, N., Matthiessen, J., McInroy, D., Moore, T.C., Onodera, J., O'Regan, M., Pälike, H., Rea, B., Rio, D., Sakamoto, T., Smith, D.C., Stein, R., St John, K., Suto, I., Suzuki, N., Takahashi, K., Watanabe, M., Yamamoto, M., Farrell, J., Frank, M., Kubik, P., Jokat, W. & Kristoffersen, Y. 2006: The Cenozoic palaeoenvironment of the Arctic Ocean. *Nature 441,* pp. 601–605. https://doi.org/10.1038/nature04800

Müller, D.R. & Spielhagen, R.F. 1990: Evolution of the Central Tertiary Basin of Spitsbergen: towards a synthesis of sediment and plate tectonic history. *Palaeogeography, Palaeoclimatology, Palaeoecology 80,* pp. 153–172. https://doi.org/10.1016/0031-0182(90)90127-S

Myhre, A.M. & Eldholm, O. 1988: The western Svalbard margin (74°–80°N). *Marine and Petroleum Geology 5,* pp. 134–156. https://doi.org/10.1016/0264-8172(88)90019-0

Nanson, G. & Croke, J.C. 1992: A genetic classification of floodplains. *Geomorphology 4*, pp. 459–486. https://doi.org/10.1016/0169-555X(92)90039-Q

Nøttvedt, A., Livbjerg, F., Midbøe, P.S. & Rasmussen, E. 1993: Hydrocarbon potential of the Central Spitsbergen Basin. *Norwegian Petroleum Society, Special Publications 2*, pp. 333–361. https://doi.org/10.1016/B978-0-444-88943-0.50026-5

Oakey, G.N. & Chalmers, J.A. 2012: A new model for the Paleogene motion of Greenland relative to North America: Plate reconstructions of the Davis Strait and Nares Strait regions between Canada and Greenland. *Journal of Geophysical Research: Solid Earth 117,* pp. 1–28. https://doi.org/10.1029/2011JB008942

Oreshkina, T. V 2012: Evidence of Late Paleocene – Early Eocene hyperthermal events in biosiliceous sediments of Western Siberia and adjacent areas. *Austrian Journal of Earth Sciences 105,* pp. 145–153.

Osmundsen, P.T. & Andersen, T.B. 2001: The middle Devonian basins of western Norway: Sedimentary response to large-scale transtensional tectonics? *Tectonophysics 332*, pp. 51–68. https://doi.org/10.1016/S0040-1951(00)00249-3

Osmundsen, P.T. & Péron-Pinvidic, G. 2018: Crustal-Scale Fault Interaction at Rifted Margins and the Formation of Domain-Bounding Breakaway Complexes: Insights From Offshore Norway. *Tectonics 37*, pp. 935–964. https://doi.org/10.1002/2017TC004792

Paech, H.-J. 2001: Compressive Structures in the Central Basin, Spitsbergen. *Geologisches Jahrbuch B,* pp. 413–446.

Paech, H.-J. & Koch, J. 2001: Coalification in Post–Caledonian Sediments on Spitsbergen. *In:* Tessensohn, F. (ed.): *Intra-Continental Fold Belts: CASE 1, Spitsbergen*, Schweizerbart Science Publishers, pp. 507–530.

Passchier, C.W. & Trouw, R.A.J. 2005: *Microtectonics.* Springer-Verlag Berlin Heidelberg.

Peron-Pinvidic, G., Manatschal, G. & Osmundsen, P.T. 2013: Structural comparison of archetypal Atlantic rifted margins: A review of observations and concepts. *Marine and Petroleum Geology 43,* pp. 21–47. https://doi.org/10.1016/j.marpetgeo.2013.02.002

Piepjohn, K., von Gosen, W. & Tessensohn, F. 2016: The Eurekan deformation in the Arctic: an outline. *Journal of the Geological Society 173*, pp. 1007–1024. https://doi.org/10.1144/jgs2016-081

Postma, G., Nemec, W. & Kleinspehn, K.L. 1988: Large floating clasts in turbidites a mechanism for their emplacement. *Sedimentary Geology 58,* pp. 47–61. https://doiog/10.1016/00370738(88)90005-X

Ramsay, D.M. 1964: Deformation of Pebbles in Lower Old Red Sandstone Conglomerates Adjacent to the Highland Boundary Fault Deformation of Pebbles in Lower Old Red Sandstone. *Geological Magazine 101,* pp. 228–248. https://doi.org/10.1017/S0016756800049463

Ritzmann, O., Jokat, W., Czuba, W., Guterch, A., Mjelde, R. & Nishimura, Y. 2004: A deep seismic transect from Hovgård Ridge to northwestern Svalbard across the continental-ocean transition: A sheared margin study. *Geophysical Journal International 157,* pp. 683–702. https://doi.org/10.1111/j.1365-246X.2004.02204.x

Rust, B.R. 1972: Structure and Process in a Braided River. *Sedimentology 18,* pp. 221–245. https://doi.org/10.1111/j.1365-3091.1972.tb00013.x

Rye-Larsen, M. 1982: *Svalbard's Vestmargin, Forlandsundet Graben - Sedimentasjon og tektonisk utvikling av et bassemg ved en transform plategrense.* Unpublished Candidatus Mag thesis, University of Bergen, 380 pp.

Scheiber, T., Viola, G., van der Lelij, R., Margreth, A. & Schönenberger, J. 2019: Microstructurally-constrained versus bulk fault gouge K – Ar dating. *Journal of Structural Geology 127*, pp. 1–14. https://doi.org/10.1016/j.jsg.2019.103868

Schneider, D., Faehnrich, K., Majka, J. & Manecki, M. 2018: Ar / 39 Ar geochronologic evidence of Eurekan deformation within the West Spitsbergen Fold and Thrust Belt. *In:* Piepjohn, K., Strauss, J. V., Reinhardt, L. & McClelland, W.C. (eds.): *Circum-Arctic Structural Events: Tectonic Evolution of the Arctic Margins and Trans-Arctic Links with Adjacent Orogens,* Geological Society of America Special Paper, pp. 1–16. https://doi.org/10.1130/2018.2541(08)

Schönenberger, J., van der Lelij, R., Xie, R., Schaaf, N.W. & Osmundsen, P.T. 2019: Unravelling the timescales and conditions of clay forming processes with X–Ray diffraction and K–Ar analysis. *Geological Society of Norway, Winter Conference 2019, 7–9 January.* Bergen.

Schumacher, E. 1975: Herstellung von 99,9997% 38Ar für die 40K/40Ar Geochronologie. *Geochronologia Chimia 24,* pp. 441–442.

Seiler, C., Fletcher, J.M., Quigley, M.C., Gleadow, A.J.W. & Kohn, B.P. 2010: Neogene structural evolution of the Sierra San Felipe, Baja California: Evidence for proto-gulf transtension in the Gulf Extensional Province? *Tectonophysics 488*, pp. 87–109. https://doi.org/10.1016/j.tecto.2009.09.026

Senger, K., Brugmans, P., Grundvåg, S., Jochmann, M., Nøttvedt, A., Olaussen, S., Skotte, A. & Smyrak-Sikora, A. 2019: Petroleum, coal and research drilling onshore Svalbard: a historical perspective. *Norwegian Journal of Geology 99,* pp. 1–30. https://doi.org/10.17850/njg99-3-1

Skogseid, J., Planke, S., Faleide, J.I., Pedersen, T., Eldholm, O. & Neverdal, F. 2000: NE Atlantic continental rifting and volcanic margin formation. *Geological Society, London, Special Publications 167,* pp. 295–326. https://doi.org/10.1144/GSL.SP.2000.167.01.12

Sperling, V. 1990: *Kartierung der tertiären Ablagerungen auf Sarsøyra, Oscar II Land, Spitsbergen, Svalbard.* Unpublished diploma thesis, Universität Hamburg.

Spielhagen, R.F. & Tripati, A. 2009: Evidence from Svalbard for near-freezing temperatures and climate oscillations in the Arctic during the Paleocene and Eocene. *Palaeogeography, Palaeoclimatology, Palaeoecology 278,* pp. 48–56. https://doi.org/10.1016/j.palaeo.2009.04.012

Steel, R.J., Gjelberg, J.G., Helland-Hansen, W., Kleinspehn, K.L., Nøttvedt, A. & Rye-Larsen, M. 1985: The Tertiary Strike-Slip Basins and Orogenic Belt of Spitsbergen. *In:* Biddle, K.T. & Christie-Blick, N. (eds.): *Glossary – Strike-Slip Deformation, Basin Formation, and Sedimentation,* pp. 339–359. https://doi.org/10.2110/pec.85.37.0339

Steiger, R.H. & Jäger, E. 1977: Subcommission on geochronology: convention on the use of decay constants in geo-and cosmochronology. *Earth and Planetary Science Letters 36,* pp. 359–362. https://doi.org/10.1016/0012-821X(77)90060-7

Sutherland, F.H., Kent, G.M., Harding, A.J., Umhoefer, P.J., Driscoll, N.W., Lizarralde, D., Fletcher, J.M., Axen, G.J., Holbrook, W.S., González-Fernández, A. & Lonsdale, P. 2012: Middle Miocene to early Pliocene oblique extension in the southern Gulf of California. *Geosphere 8,* pp. 752–770. https://doi.org/10.1130/GES00770.1

Tessensohn, F. & Piepjohn, K. 2000: Eocene compressive deformation in Arctic Canada, North Greenland and Svalbard and its plate tectonic causes. *Polarforschung 68*, pp. 121–124.

Traverse, A. 2007: *Paleopalynology. Vol 28.* Springer Science & Business Media, 812 pp. https://doi.org/10.1007/978-1-4020-5610-9

Venkat-Ramani, M. & Tikoff, B. 2002: Physical models of transtensional folding. *Geology 30,* pp. 523–526. https://doi.org/10.1130/0091-7613(2002)030%3C0523:PMOTF%3E2.0.CO;2

Viola, G., Scheiber, T., Fredin, O., Zwingmann, H., Margreth, A. & Knies, J. 2016: Deconvoluting complex structural histories archived in brittle fault zones. *Nature Communications 7*, pp. 1–10. https://doi.org/10.1038/ncomms13448

Viola, G., Torgersen, E., Mazzarini, F., Musumeci, G., van der Lelij, R., Schönenberger, J. & Garofalo, P.S. 2018: New constraints on the evolution of the inner Northern Apennines by K-Ar dating of Late Miocene-Early Pliocene compression on the Island of Elba, Italy. *Tectonics 37,* pp. 3229–3243. https://doi.org/10.1029/2018TC005182

Vogt, P.R. & Parrish, M. 2012: Driftwood dropstones in Middle Miocene Climate Optimum shallow marine strata (Calvert Cliffs, Maryland Coastal Plain): Erratic pebbles no certain proxy for cold climate. Palaeogeography, Palaeoclimatology, Palaeoecology 323, pp. 100–109. https://doi.org/10.1016/j.palaeo.2012.01.035

von Gosen, W. & Paech, H.-J. 2001: Structures in the Tertiary sediments of the Forlandsundet Graben. *In:* Tessensohn, F. (ed.): *Intra-Continental Fold Belts: CASE 1, Spitsbergen,* Schweizerbart Science Publishers, pp. 475–502.

Walker, R.G. & Cant, D.J. 1984: Facies Model – 3. Sandy fluvial systems. *Geoscience Canada 3*, pp. 71–89.

Worsley, D. 2008. The post–Caledonian development of Svalbard and the western Barents Sea. *Polar Research 27,* pp. 298–317. https://doi.org/10.1111/j.1751-8369.2008.00085.x